AN ABSTRACT OF THE THESIS OF

James Rossi for the degree of Master of Science in Biochemistry and Biophysics presented on March 6, 1997. Title: Biosynthetic Investigations of Two Secondary Metabolites from the Marine Cyanobacterium *Lyngbya majuscula*

Abstract approved:

Redacted for Privacy

William H. Gerwick

Marine cyanobacteria have been shown to produce a variety of biologically active and stucturally diverse secondary metabolites. These compounds are of interest to natural products researchers mainly because of their potential application as biomedicinals, biochemical probes, and agrichemicals.

The metabolic pathways utilized by the cyanobacterium *Lyngbya majuscula* to generate curacin A, a potent antimitotic and its cometabolite, the molluscicidal barbamide, have been studied. Application of methods including radioisotope and stable isotope labeling have revealed the role of acetate and the amino acids methionine, valine, cysteine, and leucine as potential precursors in the biosynthesis of curacin and barbamide.

An analytical technique based upon GC-EIMS methodology has also been developed to monitor the production levels of curacin A from cultures of *Lyngbya majuscula* with respect to growth. This method which makes use of the thiazole analog of curacin A, curazole as an internal standard, has also been preliminarily applied to the curacin A production in response to enviromental factors associated with changes in geographical locations at or near sites where the original collections of the cyanophyte

were made in Curaçao, Netherlands Antillies. This was performed by a series of transplantation experiments envolving high and trace curacin A producing strains of *L. majuscula.*

Interest in the bioactive profile of curacin A prompted a pilot scale up of the cultured tissue for isolation of the metabolite. These efforts provided a framework of methods that can be used industrially to obtain large quantites of the compound to meet possible future pharmaceutical or dignostics demands.

Biosynthetic Investigations of Two Secondary Metabolites from the Marine Cyanobacterium *Lyngbya majuscula*

by

James V. Rossi

A THESIS

submitted to

Oregon State University

in partial fulfillment of

the requirements for the

degree of

Master of Science

Presented March 6, 1997

Commencement June 1997

Master of Science thesis of James Rossi presented on March 6, 1997

APPROVED:

Redacted for Privacy

Major Professor, representing Biochemistry and Biophysics

Redacted for Privacy

Chairman of the Department of Biochemistry and Biophysics

Redacted for Privacy

Dean of the Graduate School

I understand that my thesis will become part of the permanent collection of Oregon State University Libraries. My signature below authorizes release of my thesis to any reader upon request.

Redacted for Privacy

James V. Rossi, Author

ACKNOWLEDGEMENTS

I thank Dr. William Gerwick for his kind support and guidance throughout my research studies at Oregon State. He has been an inspiration as a mentor and a friend.

My gratitude also goes to my friend and labmate Mary Ann Roberts who's talents as a blue-green culturalist have been essential to my research.

I would like to acknowledge Brian Arbogast for FAB MS acquisition, Rodger Kohnert and Victor Hsu's laboratory for assistance with NMR experiments, Dr. Mark Zabriskie and Dr. Phil Proteau for lots of helpful suggestions and information. Special thanks to Ivan Negelkirken at CARMABI for assistance with ecological experiments.

My fellow labmates have been a great source of support, camaraderie, and insightful discourse. I am grateful for all of their encouragement and good humor.

My admiration and appreciation go to my mate, Pam who has shown a great deal of interest in my research and has helped proofread this manuscript.

I would finally like to give my warmest thanks to my mother, father, and grandmother who were my first science teachers and have stood behind me with love and confidence.

CONTRIBUTION OF AUTHORS

Dr. Philip J. Proteau and Dr. William Gerwick were involved in the design, analysis, and writing of the manuscript which appears in Appendix A. All analytical work was performed in the laboratory of Dr. William Gerwick who also assisted in interpretation of the data.

TABLE OF CONTENTS

LIST OF FIGURES

LIST OF FIGURES (Continued)

LIST OF ABBREVIATIONS

NMR	Nuclear Magnetic Resonence
GC-EIMS	Gas Chromatography-Electron Impact Mass Spectrometry
FAB-MS	Fast Atom Bombardment Mass Spectrometry
HPLC	High Performance Liquid Chromatography
HMBC	Heteronuclear Multiple Bond Correlation Spectroscopy
UV	Ultraviolet
TLC	Thin Layer Chromatography
TCA	Tricarboxylic Acid
NCI	National Cancer Institute
CARMABI	Caribbean Marine Biological Institute

BIOSYNTHETIC INVESTIGATIONS OF TWO SECONDARY METABOLITES FROM THE MARINE CYANOBACTERIUM *LYNGBYA MAJUSCULA*

CHAPTER 1 : GENERAL INTRODUCTION

The marine environment holds some of the Earth's most unique ecosystems. The organisms that form communities in these systems represent biological and biochemical diversity that is without parallel on land. Life forms that associate with one another through a saline aqueous medium have the potential to develop a number of chemical mechanisms with which they can communicate. This interaction may have evolved in response to competitive pressures, nutrient availability, predation, or reproductive advantages. Recognition of these ecosystems as a valuable new resource in the last twenty years by natural products researchers has ushered in an era that promises the discovery of new biologically active compounds and perhaps a greater understanding of the complexities that exist in the chemical dialog among members of marine community. These goals have been increasingly realized in the elucidation of a multitude chemically diverse entities isolated from marine sponges, tunicates, mollusks, algae, bacteria, and blue-green algae (cyanobacteria). The cyanobacteria have been particularly rich in secondary metabolites that act as neurotoxins, antiinflammatory agents and antimitotic agents. Emerging with the discovery of unique chemistry from these sources has been an interest in the biogenesis of such compounds.

Cyanobacteria are classified as eubacteria and are thought to be the first organisms to develop a two stage photosystem which eventually gave rise to chloroplasts through endosymbiotic relationships with eukaryotic hosts. This concept has been supported by molecular methods involving 16S rRNA sequencing.[1] Morphologically, these organisms may be unicellular or filamentous. Many species possess the ability to fix atmospheric nitrogen which takes place in specialized cells known as heterocysts; however some genera fix nitrogen and are nonheterocystous.

The genus *Lyngbya*, which will be described in the following chapters with respect to its secondary metabolites, is comprised of over 100 species and is characterized by disc shaped cells. Trichomes of *Lyngbya* are quite similar to those of *Ocillatoria* except that they are encased in a mucilaginous sheath.[8] Reproduction in *Lyngbya* takes place by the formation of hormogonia.[9] Due to its morphological similarity to the genera *Plectonema* and *Phormidium*, *Lyngbya* has been classified into the so called PLP grouping. Recent advances in taxonomy using 16S rRNA has clarified the relatedness of each of these genera in terms of evolutionary distance. From these analysis, the three genera of the PLP group were found to each have a distinct ancestral lineage rather than a direct relationship to each other.[9]

Bioactive metabolites from cyanobacteria are widespread in nature and represent a variety of structural classes such as alkaloid, peptide, macrolide and terpene. Some of these metabolites are products of mixed biogenesis where two or more classes are apparent in one molecule. The biosynthesis of the macrolide-amide tolytoxin (**1**) (figure 1.1) from the cyanobacteria *Tolypothrix conglutinata* is illustrative of this concept.

Tolytoxin is a member of a group of cyanobacterial metabolites known as the scytophycins and has shown selective inhibitory effects on human tumor cell lines in bioassays performed at the United States National Cancer Institute (N.C.I.). Scytophycins are polyketide-derived macrolides that have been found in genera of the Scytonemataceae and Nostocaceae.[3] Tolytoxin has been determined to impart cytotoxicity by acting as a potent microfilament depolymerizing agent.[4]

Feeding studies using stable isotope labeled substrates such as [1,2-^{13}C]-acetate, [1-^{13}C,^{18}O]-acetate, [2-^{13}C,^{15}N]-glycine and [Me-^{13}C]-methionine revealed the identity of all primary precursors in the structure. The C32 carbon chain was shown to derive from 15 acetate units condensed with glycine as the precursor to the terminal N-methyl formamide portion. [Me-^{13}C]-methionine was incorporated into 14 sites on the parent structure including the epoxide and aldehyde moieties.[2]

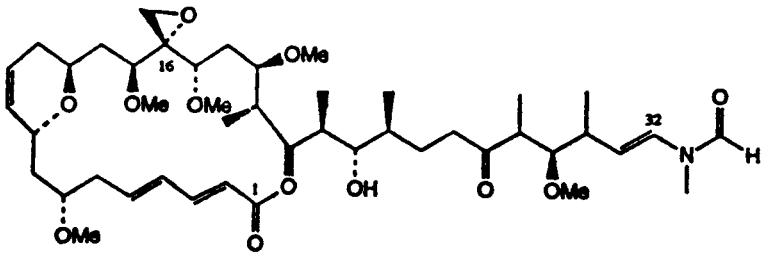

1

Tolytoxin

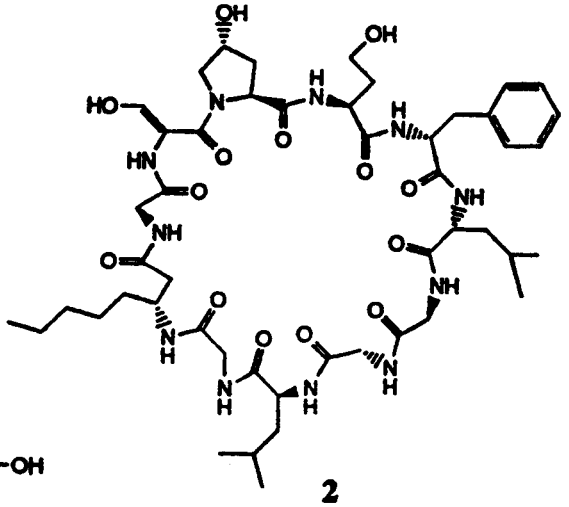

2

Hormothamnin A

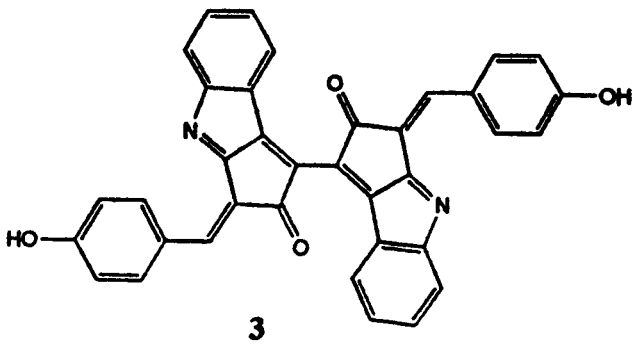

3

Scytonemin

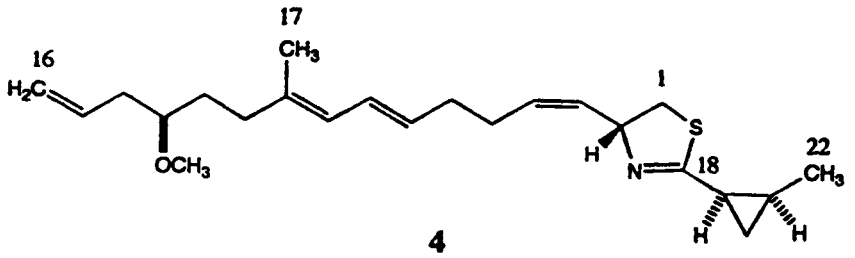

4

Curacin A

Figure 1.1 Structures of bioactive compounds from cyanobacteria

The focus in our laboratory on marine organisms, specifically cyanobacteria, has led to the discovery of several natural products from *Lyngbya majuscula*, for example, the cyclic peptide, hormothamnin A[5] (**2**) from *Hormothamnion enteromorphoides*, and the indole alkaloid scytonemin[6] (**3**) from a *Scytonema* species. Hormothamnin A, a cyclic undecapeptide was isolated through the use of bioassay guided fractionation. The compound posseses antimicrobial activity toward gram positive bacteria which aided in identifying the fractions that contained hormothamnin A from the crude lipid extract. Hormothamnin A was found to contain several nonstandard or modified amino acid residues such as L-homoserine, *allo*-isoleucine, Z-didehydrohomoalanine, hydroxyproline and β-D-aminooctanoic acid (D-BAOA). Several cyclic peptides that are produced by cyanobacteria seem to share a common structural theme in the presence of a β-amino acid with a large structurally unique side chain. Peptide toxins of microbial origin are of further interest because the gene clusters responsible for their biosyntheses are modular and peptide assembly is nonribosomally mediated. This is in contrast to the processes by which vascular plants and mammals generate peptides. In addition, both D and L isomers of standard amino acid residues may occur in microorganisms.

The sunscreen pigment scytonemin is an alkaloid dimer of units which are likely to derive from tryptophan and tyrosine. The planar structure resulting from the aromatic components and the uniformity of sp^2 hybridization throughout the molecule, absorbs light strongly in the UV A (λ_{max} =370 nm) region. Many filamentous species of cyanobacteria (including some varieties of *Lyngbya*) produce scytonemin in their sheaths as a photoprotectorant. This feature is likely to have evolved around 0.5-2.5 billion years ago in response to high UV incidence on the earth's surface.

Through collaboration with Robert Jacobs at the University of California at Santa Barbara, scytonemin was found to have anti-inflammatory properties as demonstrated in the mouse ear edema assay.[7] The mechanism of this activity appears to result from the inhibition of the enzyme PLA_2 which in mammals catalyzes one of the initial reactions in the release of lipid progenitors to endogenous proinflammatory agents.

Synthetic modifications on scytonemin have been performed in order to alter its biological and physical properties (see appendix B).

Natural product surveys conducted on coastal marine algae of the Caribbean by our laboratory have shown the filamentous cyanobacterium *Lyngbya majuscula* to be particularly rich in bioactive secondary metabolites. The lipid curacin A (**4**) was isolated from extracts of *L. majuscula* using bioassay guided fractionation which was based on brine shrimp toxicity. Further bioactivity profiles revealed the compound to be selectively cytotoxic to colon, renal, and breast tumor cell lines in a 60 cell line assay conducted at N.C.I.[10] Curacin A was later found to be a potent antimitotic agent. Cell death is caused by curacin A binding to tubulin thereby inhibiting the assembly of competent microtubules. Characterization of the interaction showed the compound to be a competitive inhibitor of colchicine-tubulin binding.[11] The potential application of curacin A as an anticancer agent has motivated our laboratory to generate quantities of the compound for future structure activity relationships, and to study it's biosynthesis.

Another class of structurally related metabolites from *L. majuscula* are the bioactive peptides, microcolins A-C (figure 3.5: **12-14**).[12] First discovered by Koehn in 1992, microcolins A and B were found to be cytotoxic to leukemic murine P-388 cells. The compounds also showed immunosuppressant activity in nanomolar concentrations as measured by the murine mixed lymphocyte response assay.[12]

Although no formal biosynthetic studies have been performed on the microcolins, it seems possible that the basic parent structure is derived from the peptide; pro-pro-val-val-leu, condensed with a lipid component (possibly a tetraketide) to form the N29 amide.

We propose that curacin A is a product of mixed biogenesis involving polyketide and amino acid metabolism. The biomedicinal importance of peptide and polyketide derived natural products from microorganisms has provided the impetus to explore these pathways in detail. Macrolide, aromatic, and heterocyclic antibiotics emanating from polyketide pathways by microorganisms, have been determined to arise from Claisen condensation of acetate (and sometimes propionate) units activated at the carboxyl group as coenzyme A thioesters.[13] The process is initiated by the condensation of acetyl-SCoA

with malonyl-SCoA. Chain elongation occurs analogously to fatty acid biosynthesis with the exception that addition of a new acetate unit proceeds without reduction of the previous carbonyl group. Resulting carbon skeletons will then bare various oxo centers that are somewhat reactive and available for further modification such as methlyation or folding within the chain to form cyclic structures. This factor is what allows the great diversity of polyketide metabolites that are of current medicinal interest.

The arrangement of both polyketide and polypeptide genes in microorganisms are modular. Each module is comprised of the gene segments required to carry out a condensation between amino acid units or acetate units. For example a tripeptide or triketide will each contain at least three modules. It is a set of modules that code for the biocatalysts which guide a metabolite precursor through the steps to completion of the target compound.[14]

Often the production of certain toxins by cyanobacteria have posed public health concerns. Examples include the hepatotoxic cyclic peptide microcystin-LR (**5**) and neuromuscular toxic alkaloids produced by *Anabaena.* These compounds are water soluble and are associated with blooms of algae usually resulting from nutrient fluctuations in freshwater environments.

The tropane-type alkaloid anatoxin-a (**6**)[15,16] is produced by *Anabaena flos-aquae* and has been responsible for the poisoning of dogs in Scotland and cattle in southern Canada. Toxicity results from neuromuscular blockage cause by postsynaptic binding of the ligand to nicotinic and muscarinic receptors in mammals.

Studies on the biosynthesis of anatoxin-a have shown the heterocyclic portion of the pyrrolidine ring to originate from putrescine via ornithine decarboxylase.[15] In this investigation, the notion that secondary metabolism in cyanobacteria is plasmid linked

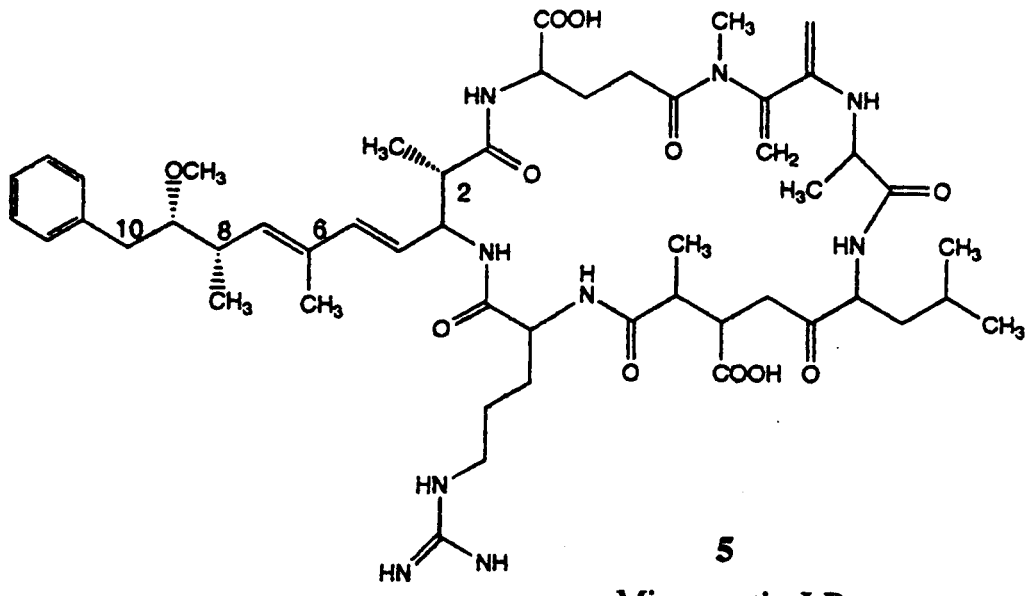

5

Microcystin-LR

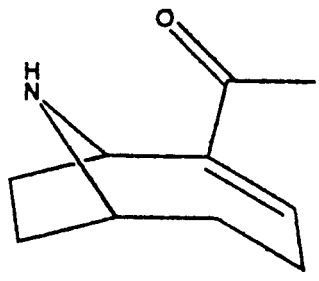

6

Anatoxin-A

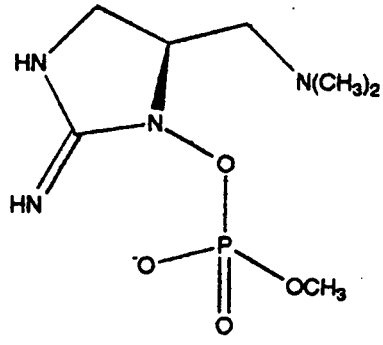

7

Anatoxin-A(s)

Figure 1.2 Environmental toxins from cyanobacterial species

was partially supported by the detection of plasmid DNA in toxin producing strains where plasmids were absent in nontoxic strains.[15]

Other strains of *Anabaena flos-aquae* produce the guanidinyl organophosphate anatoxin-a(s) (**7**) which bares little resemblance to anatoxin-a but elicits a similar biological effect. This metabolite is the only known naturally occurring organophosphate and exerts toxicity as an irreversible inhibitor of acetylcholinesterase. As a result, acetylcholine is not degraded in muscle tissue thereby causing fatigue, twitching and eventually paralysis.[16]

Microcystin-LR (**5**) from the unicellular cyanobacterium *Microcystis aeruginosa* is a protein phosphatase inhibitor which is the suspected cause of its potent hepatotoxicity. Feeding studies conducted on cultured *Microcystis aeruginosa* have established the amino acid precursors to the cyclic peptide as well as the uncommon (2S,3S,8S,9S)-3-amino-9-methoxy-2,6,8-trimethyl-10-phenyl-4,6-decadienoic acid (Adda) substructure.[17] The amino acids L-glu, N-Me dehydroalanine, L-ala, L-leu, 3-methylaspartate and, L-arg comprise the peptide ring in addition to Adda which originates from the polymerization of 4 acetate units, with the phenyl ring from L-phe. Methylation of sites 2, 6, and 8 of Adda were found to be introduced via S-adenosyl methionine (SAM).[17]

The studies of biosynthesis in the above cases were facilitated by the use of stable isotope (^{13}C, ^{2}H and ^{18}O) NMR. Early investigations which utilized radioisotopically labeled precursors depended largely on laborious chemical degradative processes in order to localize the labels. NMR studies using ^{13}C labeled precursors allow the entire sample to be studied intact for the determination of enrichment of the carbon chain due to direct uptake of a labeled substrate. Labeling patterns are often viewed in the NMR spectra as a marked signal increase over natural abundance (^{13}C natural abundance = 1.1%) or by signal splitting due to carbon-carbon coupling. From these observations biogenic precursors can be structurally assigned to parts of a natural product of interest.

The following chapters discuss the procedures and results involved in characterizing the tropical cyanobacterium *Lyngbya majuscula* with respect to the

production of curacin A (**4**) (figure 1.1) and its co-metabolite, barbamide (**3**) (figure 2.1) in culture and in the field. Profiles of culture growth and metabolite production were used as a background for biosynthetic studies on the cyanobacterial metabolites, curacin A and barbamide, which are explained in subsequent chapters.

CHAPTER 2: CHARACTERIZATION OF CURACIN A PRODUCTION BY CULTURED AND FIELD COLLECTED ISOLATES OF *LYNGBYA MAJUSCULA*

Abstract

The marine cyanobacterium, *Lyngbya majuscula* was originally collected from Curaçao and has now been maintained in culture by our laboratory for four years. Several strains which produce the biologically active compound curacin A have been evaluated for growth properties and metabolite generation. An analytical method which uses a curacin A analog as an internal standard was developed and has been implemented in describing one strain with respect to growth and curacin A production characteristics. This method has also been applied to ecological studies on field collected samples to investigate the effect of habitat on curacin A production. Finally, cultures of *L. majuscula* have been scaled up in order to study the dynamics of large scale tissue generation and to produce quantities of the metabolite to meet future demand for biological studies.

Introduction

Exploration of pathways that lead to secondary metabolites in microorganisms require that the producer strain be maintained in stable culture and reliably express the desired chemistry over time. Knowledge of production levels and the timing of biosynthesis are central in such studies. Other aspects of culture conditions such as light, medium components, and salinity may also affect secondary metabolism and should be evaluated.

In working with *Lyngbya majuscula,* which in its native habitat produces curacin A (**1**) and barbamide (**3**), it was necessary to first show that cultures derived from field collections newly synthesize these compounds in reasonable quantities.

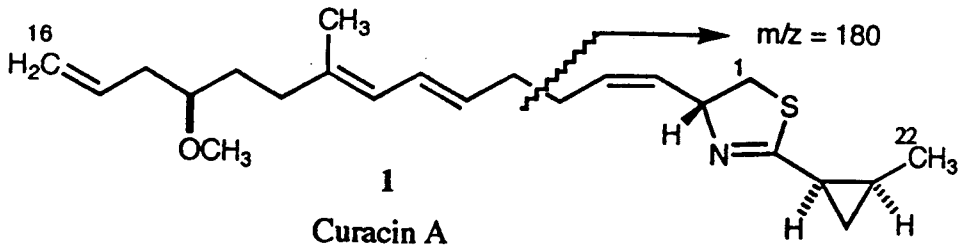

1

Curacin A

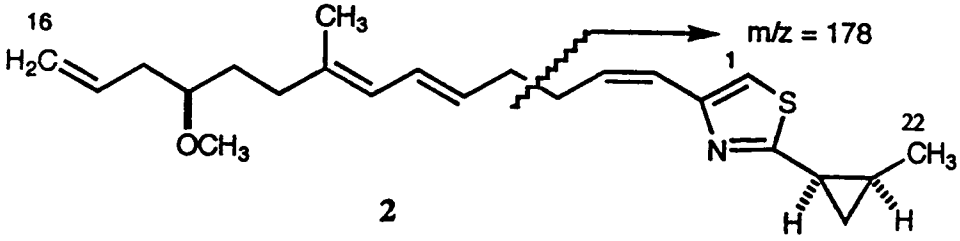

2

Curazole

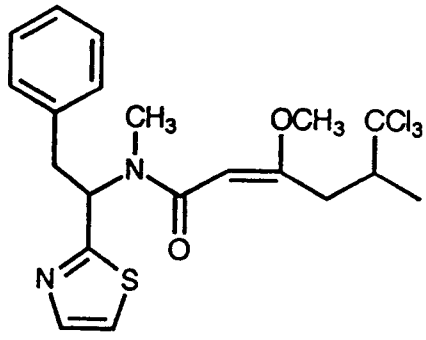

3

Barbamide

Figure 2.1 Structures of curacin A, curazole and barbamide

Lyngbya majuscula was first collected in a 1991 algal survey which took place on coastal sandy regions and mangrove environments of the island of Curaçao. Following the discovery of curacin A, the cyanobacterium was recollected and successfully cultured in 1993. Cultures of the alga have been maintained in our laboratory since that time without perceivable loss of curacin A production. However production levels from strains generated by subculturing have been somewhat variable.

A gas chromatography-electron ionization mass spectrometry (GC-EIMS) based analytical method was designed to monitor production of curacin A as a function of various culture growth conditions. Curazole (**2**), a synthetically derived analog of curacin A, was used in the analysis as an internal standard from which levels of curacin A occurring in tissue were determined.

The selection and characterization of an optimum strain of *Lyngbya majuscula* was required to conduct reliable biosynthetic studies. Twenty-nine subcultures have been generated from three Curaçao collections of the cyanobacterium and were assessed using the analytical method described herein. We found a strain that grew well and faithfully produced curacin A at levels desirable for both biosynthetic and scale-up studies. Cultures of the optimum strain yielded extracts that were analyzed to generate a profile of curacin A biosynthesis as a function of culture age. This isolate also exhibited barbamide production. Information from this study was later used to time precursor feedings aimed at the pathway elucidation of curacin A and barbamide.

Chemical adaptation by cyanobacteria in the marine environment may occur as a response to grazing pressures, microbial infestations, or competition by other organisms for available settling space. The island of Curaçao posseses a variety of coastal habitats where *L. majuscula* can be found. Collection and extraction of the cyanobacterium from several of these sites have shown the organism to exhibit different chemotypes. Extracts from some strains contain malyngamide or microcolin chemistry while others contains curacin A and possibly barbamide. Whether this variation indicates a fundamental genetic difference between strains or a system that is susceptible to regulation upon exposure to

environmental factors was preliminarily studied. In May of 1996 on a collection expedition to the Netherlands Antilles, we revisited three sites in Curaçao where *L. majuscula* was first obtained. These were the shallow water, sand and rock environments of CARMABI and Las Palmas, and the inland mangrove habitat of Santa Barbara. A fourth site, Vredenberg also was visited. Here a new collection was made of a deeper water variant that produces only trace amounts of curacin A. Transplants were made of the low level producer from its native habitat to environments where *L. majuscula* usually contains high quantities of curacin A. Reciprocal transplants and control experiments were also conducted. After a six week period, these transplants were shipped to our lab in Oregon for evaluation. Using the curazole analytical method, extracts of the transplants were analyzed. Although growth of the low level producer (Vredenberg) was robust, no evidence of upregulation with respect to curacin A production was observed. These ecological studies give preliminary insight into the nature of chemotypic variance of *L. majuscula* in the field.

In 1991 a *Lyngbya* sp. was cultured for the study of it's production of compounds that were known to be cytotoxic to murine p-388 leukemia cells.[18] Researchers at Harbor Branch Oceanographic Institute grew *Lyngbya* "pearl strain" in a 250 L bioreactor and investigated the correlations between culture growth time and cytotoxicity of extracts taken at several time points. Over a 190 hour culture cycle, the pearl strain *Lyngbya* produced the bioactive agents between 0-62 hrs and 142-190 hrs. The intervening period, 63-141 hrs was marked by a lack of detectable cytotoxicity of the extracts. This temporal separation of bioactivity was speculated to result from the production of two different compounds.[18]

In recent years following the discovery of curacin A, there has been increased interest in the drug's potential for diagnostic, biochemical and *in vivo* studies. Chemical synthesis of curacin A has been achieved, but in all cases requires a multiple step approach.[19] Even with the best methods giving a yield of 12%, it unlikely that the processes are of industrial utility.[20-25] This need has prompted our lab efforts to biosynthetically generate enough of the compound for use in collaborative endeavors. The

study provided a way to gauge the biosynthetic potential of both the organism and our facilities and to identify the problems associated with large scale culture.

Scale-up of four batch cultures of *L. majuscula* strain 19L totaling 640 L, were grown over a six week period. Harvest and subsequent extraction of the tissue yielded the drug in moderate quantities. The study illustrated the potential application of the scale-up method to an industrial setting.

Experimental Methods

General Methods: Field collected samples of *Lyngbya majuscula* from Curaçao were brought back to Oregon and are currently maintained in culture at 28°C in salt water BG11 medium.[26] Barbamide and curacin A were shown to be present in the organic extract from the cultured organism by 2 dimensional thin layer chromatography (TLC) using 10% MeOH:$CHCl_3$ in the first and 50% EtOAc:hexanes in the second dimension. TLC plates were aluminum backed silica coated (Merck). Presence of these compounds was later confirmed by nuclear magnetic resonance (Bruker AM 400).

Calibration Curves: Curazole was prepared by manganese dioxide oxidation of curacin A by R.S. Geralds in our laboratory. Curacin A was isolated and purified as previously described. (1) Separate stock solutions of each compound were prepared from 1 μg/μL solutions in hexanes at concentrations of 10-500 ng/μL by serial dilution. One microliter of each including the original stock solution was injected in duplicate onto the GC-MS. (Hewlett-Packard model 5890 series II connected to a Hewlett-Packard model 5971 mass spectrometer). Total ion and ion extraction (m/z = 180 : curacin A, m/z = 178 : curazole) peak areas were calculated and plotted for each concentration (Kaleidagraph). Analysis of unknowns gave ion abundances for curacin A and curazole which were converted to actual injected quantities of these compounds through application of linear

relationships A and B. Using these values and the quantity of curazole added (X_A) at the time of extraction, the curacin A content of the extract (Z_A) was determined from the proportional relationship C.

A. Linear equation for curacin A detector response

$W = -1.79x10^6 + 54497(Z_B)$ $R = 0.99$

where W = area measured by gc-eims and Z_B = curacin A detected

B. Linear equation for curazole detector response

$Y = -38358 + 13481(X_B)$ $R = 0.97$

where Y = area measured by gc-eims and X_B = curazole detected

C. Peak Ratio for curacin A and curazole

$$\frac{X_B \text{ (measured)}}{X_A \text{ (added)}} = \frac{Z_B\text{(measured)}}{Z_A\text{(tissue)}}$$

X_A = ng curazole added

X_B = ng curazole detected by gc-eims (calibration curve)

Z_A = ng curacin A present at time of extraction

Z_B = ng curacin A detected by gc-eims (calibration curve)

Tissue extraction and sample preparation: Cultures of *Lyngbya majuscula* were harvested from 250 mL Erlenmeyer flasks containing 100 mL SWBG11 medium. The tissue was blotted dry, weighed, cut into small chunks with scissors, pulverized under liquid N_2 by mortar and pestle, and extracted in 2:1 dichloromethane:methanol. Generally, blotted tissue masses of 200 mg and under only needed to be extracted once whereas those over 200 mg required multiple extractions. The extracts were gravity filtered through glass wool. Curazole (55 µL) was added to the tissue at time of solvent addition from a 1 µg/µL solution in hexane. The organic layer was collected and dried in vacuo and weighed. Two milliliters of 5% EtOAc/hexanes was used to resuspend the extract and the resulting solution was applied to a Sep-Pak cartridge (silica 500mg, Waters Co.) equilibrated in hexanes. Curacin A and curazole were collected by elution in 10 Sep-pak

volumes (30 mL total) of 5% EtOAc/hexanes. Elution with 5 volumes of 50% EtOAc/hexanes (15 mL) gave a crude second fraction containing barbamide. This elution was followed by a 100% EtOAc column wash. The 5% EtOAc/hexanes fraction was dried *in vacuo* and resuspended in hexanes. All three fractions were evaluated by TLC and showed curacin A and curazole to only be in the first fraction. The second fraction contained all of the barbamide.

Strain Selection: Twenty eight cultures in our lab were established from three distinct collection sites on the island of Curaçao, (site 'L' = Las Palmas dock; site 'C' = CARMABI dock; site 'B' = Mangroves at Barbara beach). These yielded twenty, three, and six cultures respectively. All cultures were maintained initially in 3 L Fernbach flasks with 1.5 L of SWBG11 medium at 28°C. One additional subculture had been grown at ambient temperature. Seed cultures in 100 mL SWBG11 in 250 mL Erlenmeyer flasks were derived from these stocks, grown for one week, and then inoculated into 10 L SWBG11 in 15L Nalgene PP sterilizing pans covered with gas permeable polyvinyl film (Fisher Brand).

Cell material was harvested and excess media was squeezed from the tissue. Each sample was stored under argon at -20°C in a Whirlpak until extracted. Cultures were periodically assessed during the one month growth period to evaluate morphological variations and general growth characteristics. After initial screening of the 28 strains for curacin A content, six subcultures were selected for further analysis.

The detailed study of the six strains was initiated by inoculating each into five identical 500 mL flasks containing 200 mL SWBG11. Inocula were bundles of filaments 5 cm x 4 mm (wet weight 50-75 mg). Cultures were grown at 28°C, 16/8 light/dark cycle (4.6 mmol photon sec^{-1} m^{-2}) for 18 days and then screened for curacin A content. The six cultures were harvested and extracted as before.

Tissue growth and production of curacin A: Strain 19L was innoculated into fifty 250 mL Erlenmeyer flasks each containing 100 mL SWBG11 and placed on a light table. Inocula were in bundles of filaments 5 cm x 3-4 mm each bundle weighing between 50 and 75 mg. Every third day, five randomly selected cultures were harvested by hand, blotted dry weighed, and extracted as above. These were analyzed for curacin A content using the curazole internal standard method. Standard deviations in the milligram curacin A content per gram wet weight of tissue were calculated for each group of five cultures and the data were graphed (Kaleidagraph).

Scale-up Culture production: Configuration of the scale-up cultures were four batches of sixteen 15 L pans (43 cm x 36 cm x 13 cm) each containing 10 L of SWBG11 medium at 28°C. Seed cultures for each batch (sixteen 75 mL SWBG11 in Erlenmeyer flasks) were taken from a single flask of strain 19L and grown for one week prior to inoculation. The scale-up pans were sealed with gas permeable polyvinyl film (Fisher) and put onto wire shelving illuminated by a bank of cool-white 40W fluorescent lights. For all pans, lighting was unidirectional from above. Approximately equal lighting intensities were provided for each pan using neutral density filters (tracing paper) (*ca.* 5.6 μmol photon s^{-1} m^{-2}). The four batches were grown for a six week period after which they were harvested separately. Tissue from each batch was combined, squeezed dry, weighed, placed into a sealable pouch, purged with argon and frozen at -80°C. The cell material was later lyophilized (Labconco 4.5L Freezone), weighed, placed into another sealable pouch, purged with argon and frozen at -20°C until extraction.

Tissue extraction was performed as described above with the exception that three additional organic extracts were made which were heated with occasional stirring. These heated extracts were combined with the room temperature extracts and filtered through glass wool. The organic solutions were reduced *in vacuo* and each of the four batch extracts were weighed. Stock solutions were prepared by vortexing each crude residue in 2.0 mL hexanes. A 25 μL aliquot was transferred to a vial containing 120 μg of the curazole internal standard. Each batch was analyzed for curacin A content as before. In

this case, the ion abundances were multiplied by a factor of 80 to obtain the total present in each 2.0 mL stock solution.

The four lipid extracts were combined and the curacin A was isolated by a combination of vacuum-liquid chromatography and normal phase HPLC with 4% EtOAc/hexanes as the eluent.

Ecological Studies: Transplants were made of a low producing strain from the Vredenberg (V) site to CARMABI, Las Palmas and Santa Barbara. Reciprocal transplants were also performed at the latter three sites. Controls were prepared by transplanting filaments to their native sites. The support for the transplants was a nylon poly rope (approx. 50 ft.) which ran across the sea floor underneath docks at CARMABI (C) and Las Palmas (L) or in mangroves at the Santa Barbara (B) site. A one meter vertically oriented section of rope was attached every meter along the main rope. The *L. majuscula* filaments were stabilized by intertwining them within the vertical rope sections. Each vertical support was labeled with numbered anchor line tags for identification. The study lasted six weeks. Our collaborator at the CARMABI research station, Ivan Nagelkerken collected the transplants and sent them to our lab preserved in 70% isopropanol labeled with the corresponding anchor tag number and the letter C, B, or L depending upon the transplant site. During the growth period, photos were taken each week in order to monitor the progress of each of the transplants.

Tissue extraction was performed as stated above with the following exceptions. Isopropanol (70%) was drained from the collection bottles and the solvent was removed in vacuo with addition of 100% EtOH to remove excess water. This was added to the main extract, produced as above. Filtration of the extract was done in a Buchner funnel with a paper filter (Whatman 44) under suction. The extracted tissue was dried under a hood and weighed. Extracts were then poured into a separatory funnel. After the phases had separated the organic layer was collected. The water layer was twice rinsed with CH_2Cl_2 and again the organic layer was added to the main extract. Resulting solutions were reduced to dryness *in vacuo,* weighed and resuspended in 1.0 mL of 5% EtOAC:hexanes.

Curazole (100 μg) was added to each extract and preparation of the samples by Sep-Pak chromatography yielded the curacin A containing fraction which was again reduced *in vacuo* and resuspeded in hexanes to a final volume of 2 mL. The samples were analyzed for curacin A content by GC-EIMS as before.

Results and Discussion

Calibration Curves: Calibration curves have been established for the linear portion of the MS detector response for curacin A and curazole that cover a mass range of 10-1000 and 10-100 ng per injection respectively. Data points recorded for curazole above 100 ng/μl deviated significantly from linearity and were less reproducible that those in the lower concentrations. Each compound posseses a prominent characteristic ms ion fragment which is used for detection. The spectrum of curacin A contains a base peak at $m/z = 180$ which results from a cleavage between C5 and C6. This represents the molecular mass of the bicyclic portion extended to C5. For the internal standard, the base peak at $m/z = 178$ results from the identical cleavage and is diagnostic. Using GC-EIMS, the quantities of curacin A present at the time of extraction were calculated by peak ratio of the ion abundances recorded for both compounds. This was made possible by fitting the measured areas from the m/z = 178 peak to the linear equation generated for curazole and calculating the mass in nanograms. Repeating this calculation for the measured curacin A peak (m/z = 180) generated a mass in ng for curacin A. Calibration curves for curacin A and curazole are shown in figures 2.2 and 2.3.

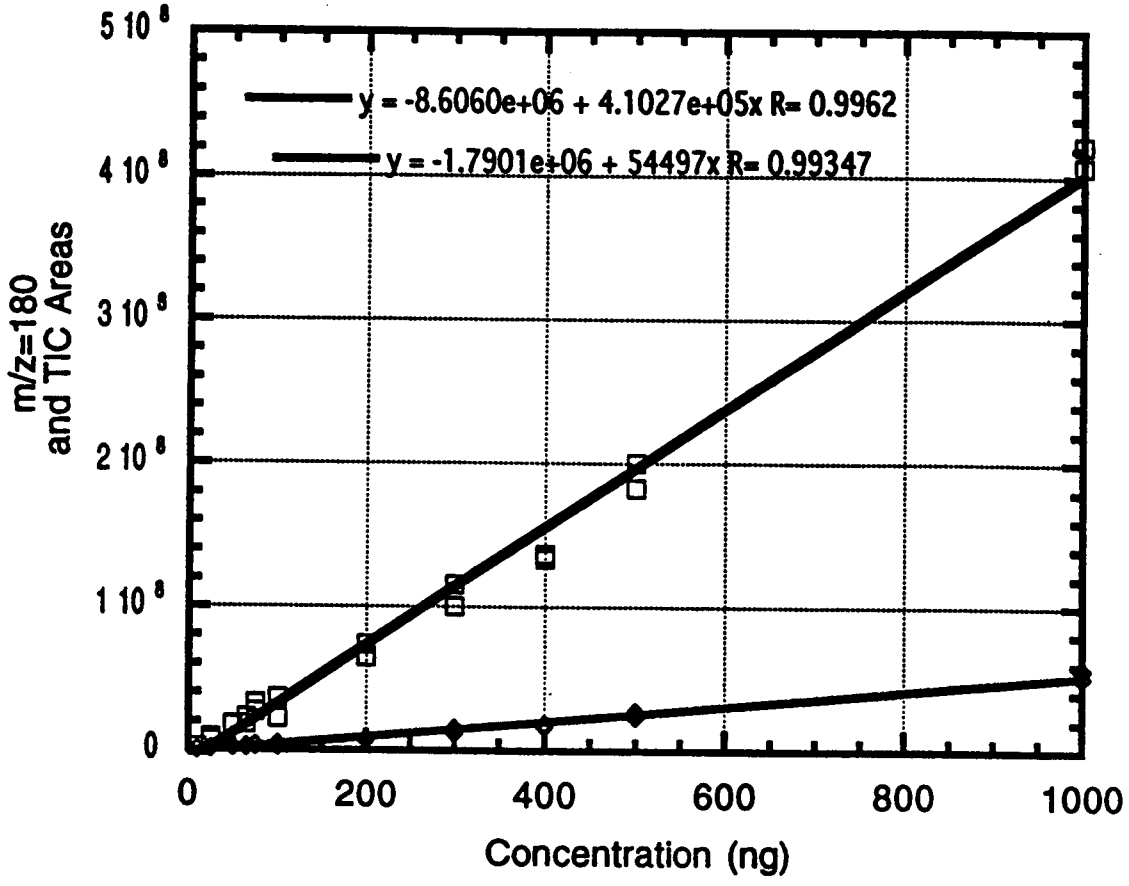

Figure 2.2 Detector response calibration curve for curacin A. Total ion chromatogram abundances or TIC are denoted by □ and abundances of m/z = 180 are denoted by diamonds.

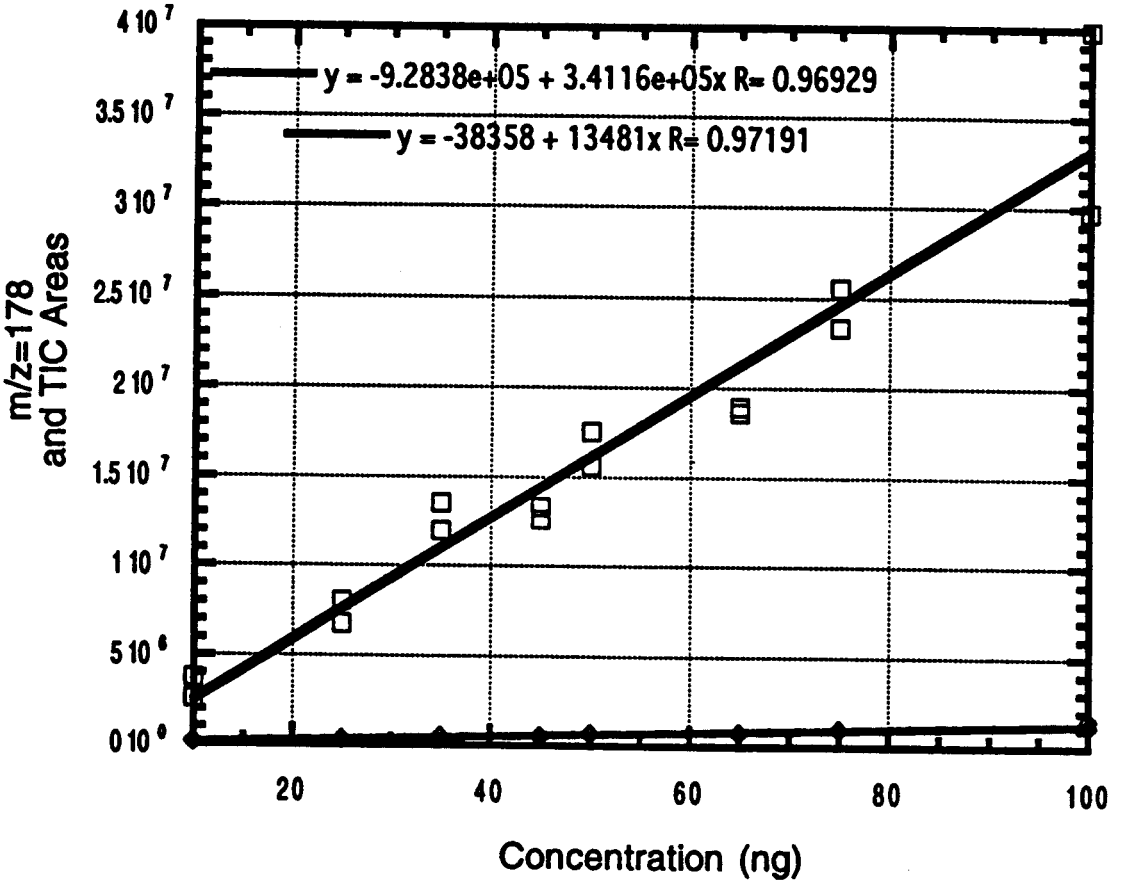

Figure 2.3 Detector response calibration curve for curazole. Total ion chromatogram abundances or TIC are denoted by □ and abundances of m/z = 178 are denoted by diamonds.

Strain analysis: The twenty-eight cultures that were grown over one month and screened for curacin A content produced between 0.4 μg to 2.8 μg per mg of algal tissue (figure 2.4). From these single point analyses, six strains were selected for more detailed analysis. Represented in this study were isolates from the three collection sites, high curacin A producers and cultures with favorable growth characteristics. Isolates 12L and 2C1 were selected because of high metabolite content. Cultures 14L and 14RT were grown at 28°C and room temperature respectively. The lush growing isolate 19L was also included in the detailed analysis. Although not a high level producer, culture 2B1 was included as a representative of the Santa Barbara collection site.

The two highest producing strains of the six were 12L at 3.61 ± 1.37 μg and 2C1 at 2.73 ± 0.41 μg curacin A per mg tissue, respectively. Both of these isolates grew quite slowly. Metabolite levels exhibited in 14L and 14RT were statistically indistinguishable. It is therefore unlikely that culture temperature has any regulatory effect on the expression level of curacin A. The Santa Barbara strain, 2B1 produced the least curacin A at 0.40 ± 0.04 mg/mg. Strain 19L maintained a combination of intermediate curacin A production (2.22 ± 0.48) with desirable growth characteristics and was therefore chosen for use in both the scale-up and biosynthetic studies. Data generated from the six strain study were plotted (Kaleidegraph) and are shown in figure 2.5.

Tissue growth and production of curacin A: Cultures of *L. majuscula* (strain 19L) were analyzed for growth and curacin A production every three days for a total of 30 days (figure 2.6). Both of these measured variables appeared to have a lag phase during the first 6 days following inoculation. The cultures then entered an accelerated growth phase for approximately 6 days during which the cell mass doubled. After the twelfth day, and continuing until the end of the 30 day period, there was no substantial increase in biomass. While inspection of the "mean algal mass" and "mean curacin A" curves in figure 2.6 suggests that production of curacin A parallels tissue growth over the first 21 days, the curacin A per milligram of tissue actually decreases throughout the culture period. At the time of inoculation (day 0), these *L. majuscula* samples contained

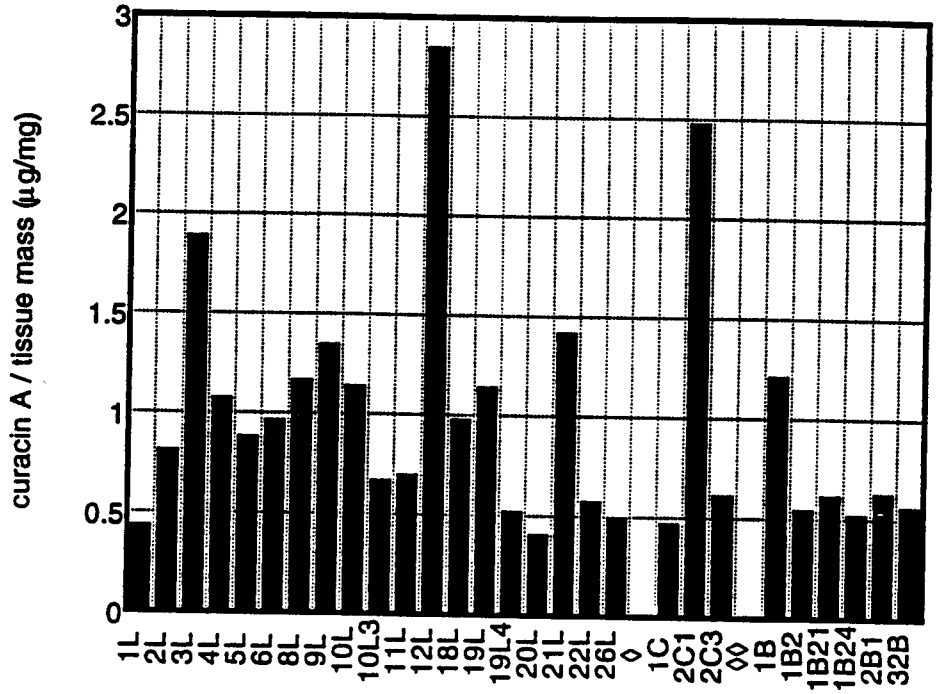

Figure 2.4 Initial culture analysis of 28 Strains of *Lyngbya majuscula* for curacin A content using the curazole internal standard method.

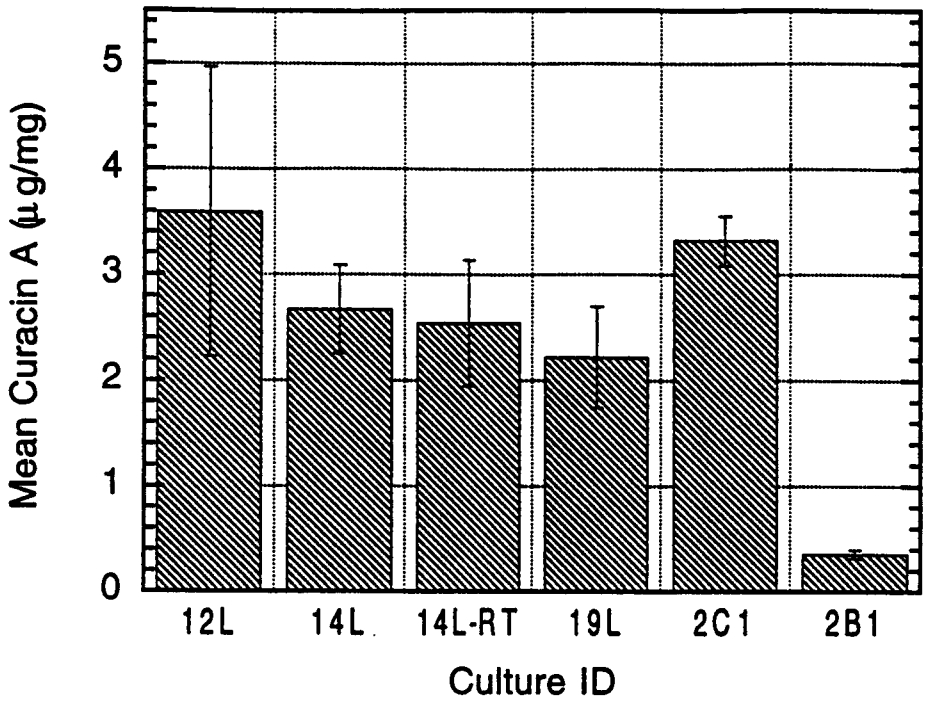

Figure 2.5 Replicate analysis of six cultured strains for curacin A content per unit of cyanobacterial mass. Error bars represent the mean of five data points.

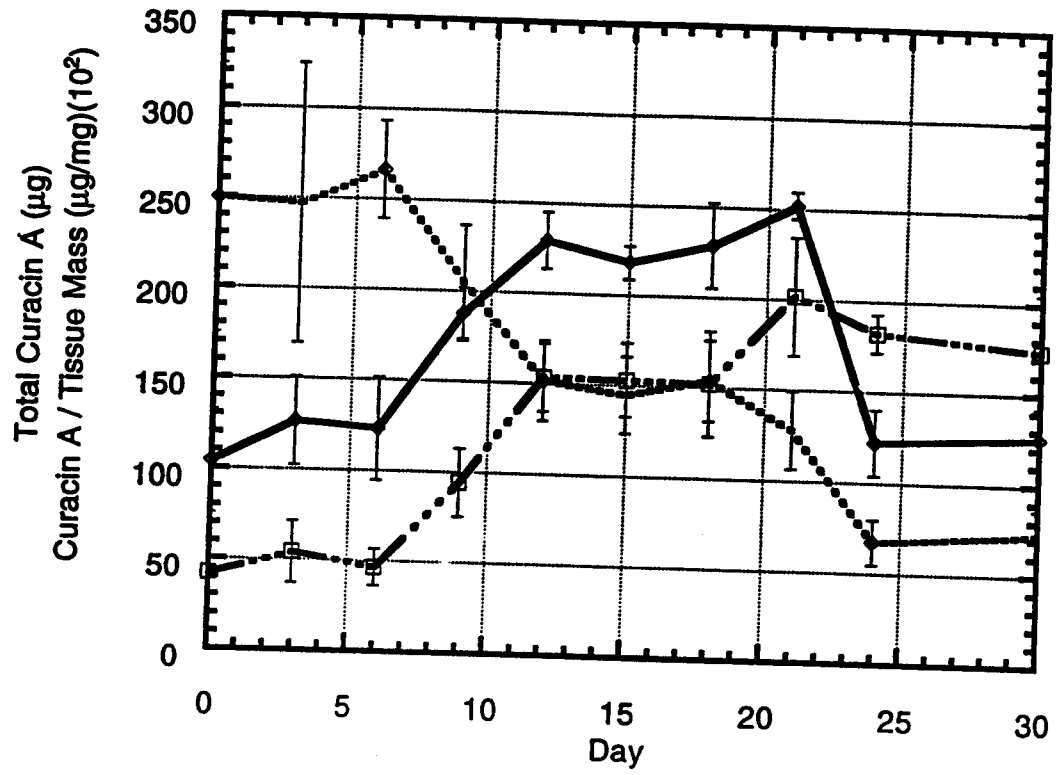

Figure 2.6 Curacin A production as a function of cultured tissue age: Filled diamonds represent the total curacin A, open boxes represent the mean total cyanobacterial mass, and open diamonds represent the mean quantity of curacin A per mg of cyanobacterial mass

2.51±0.75 μg curacin A /mg tissue whereas the cultures harvested on day 30 contained only 0.72±0.14 μg curacin A /mg tissue. These later growth stage cultures appeared to have a higher proportion of degraded trichomes.[27] Production of extracellular polysaccarides has been known to increase proportionally to cellular biomass in older cyanobacterial cultures.[28]

Scale-up Culture production: All four batches comprising a total of sixty four cultures grew well and produced significant quantities of curacin A. Three of the cultures became contaminated with an unidentified diatom species and were subsequently treated with GeO_2 (250 mg/L) which eliminated the contaminant without compromising the growth of *L. majuscula.*

Harvested tissue masses were: batch 1: 56.53 g wet, 6.04 g lyophilized; batch 2: 47.77 g wet, 4.63 g lyophilized; batch 3: 53.20 g wet, 6.22 g lyophilized; batch 4: 58.01 g wet, 6.07 g lyophilized. Analysis of the extracts for curacin A using the internal standard method gave 46.03 mg for batch 1, 27.20 mg for batch 2, 28.50 mg for batch 3, and 35.29 mg for batch 4. The total curacin A for all combined batches by the internal standard method was 137.02 mg. A total of 132.50 mg was isolated by HPLC (97% isolation efficiency) and shown to be pure by ^{1}H nmr analysis. Results for each batch are presented graphically in figure 2.7.

Several culture configurations were tried prior to this project including air bubbling in pans or flasks and shaking. Static pans provided an environment which allowed spatial dispersal of filaments in the media which may have accounted for its improved growth under these conditions. The six week scale-up culture of *L. majuscula* gave yields of curacin A and overall tissue biomass sufficient to show the utility of the method in an industrial setting.

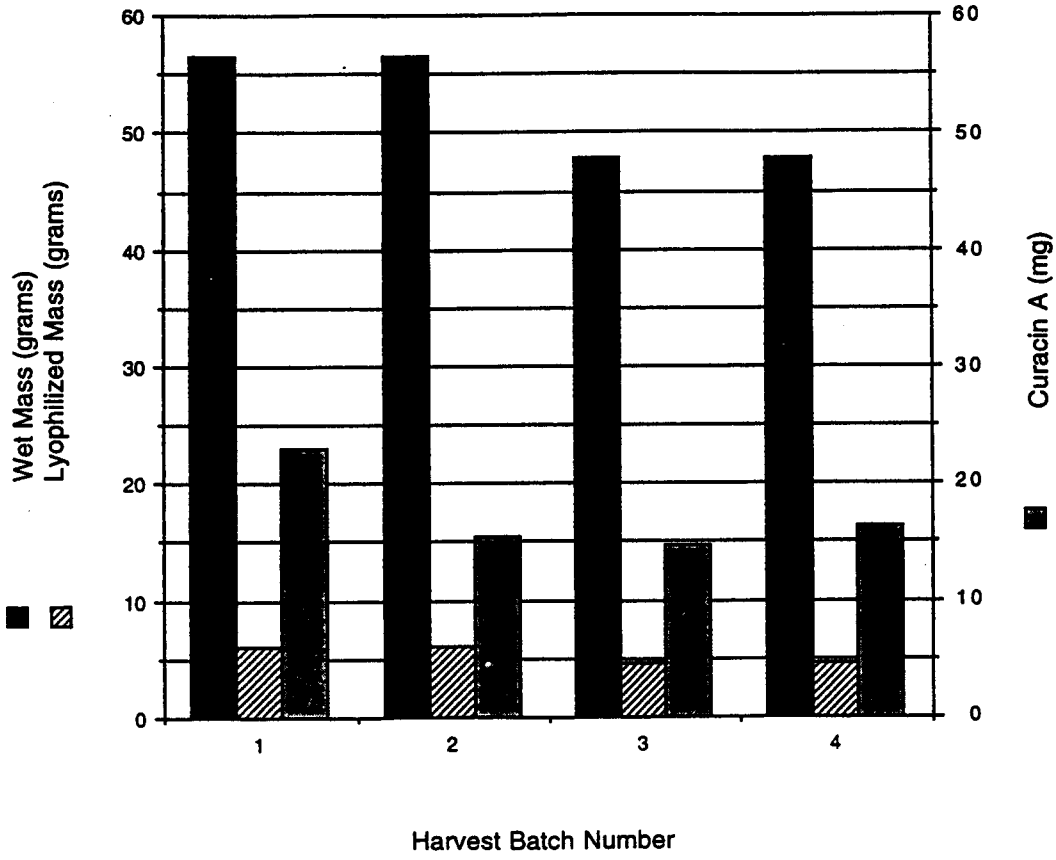

Figure 2.7 Curacin A production from four scale-up cultures of *L. majuscula*

Ecological studies: Twenty five strains originating from three sites, CARMABI, Las Palmas and Vredenberg, were transplanted to the three sites, CARMABI, Las Palmas, and Santa Barbara. Twenty three of these survived. By photographic comparison, transplants of *L. majuscula* filaments of a low curacin A producer (originating from Vredenberg) seemed to thrive in their new environments. In fact, the growth of many of the V strain transplants were visually greater than the native control and reciprocal strain transplants. This would indicate that the amount of curacin A produced by the native species is not necessarily required for successful growth in these environments. It is also likely that the process of secondary metabolite production comes at the expense of rapid tissue generation.

Analysis of the samples by GC-EIMS gave ion abundances for m/z = 178 and m/z = 180 which were converted by linear regression to quantities of curacin A and curazole. Figures 2.8 and 2.9 shows the resulting curacin A quantities which are plotted as a function of extract mass and dry tissue mass respectively. Data are grouped according to originating collection site and lettered with respect to the transplantation site. Some entries have been annotated to show the condition of the tissue or extract at the time of evaluation. A field collected sample from Vredenberg was analyzed in triplicate to establish naturally occurring levels of the metabolite from this site (NVB in Figures 2.8 and 2.9).

None of the Vredenberg samples exhibited significant elevation in curacin A production as a result of transplantation. We can assume that over the period of the experiment, no environmental stimulus such as predation, or nutrient flux, affected the metabolite production levels. Some of the reciprocal transplants also had low values when expressed with regard to dry algal mass. This is likely due to silt and sand contaminants in the samples.

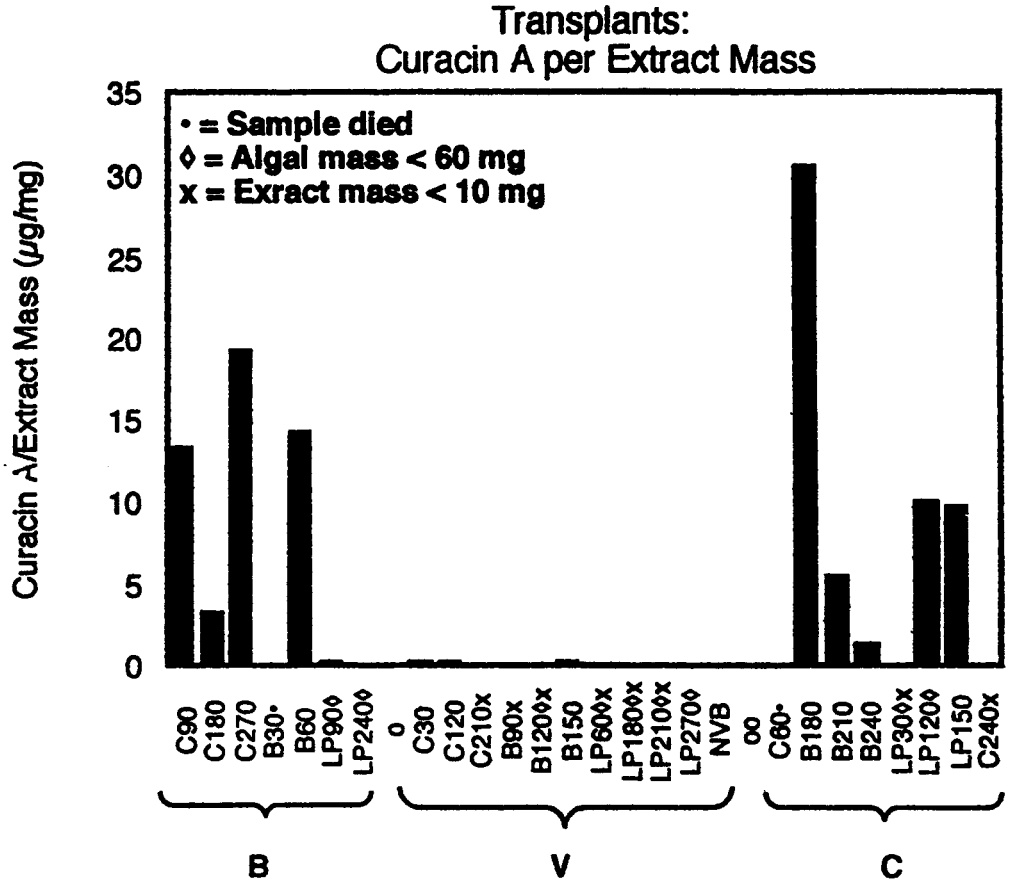

Figure 2.8 *L. majuscula* transplants: curacin A per unit of extract mass. Group B = transplants originating from Santa Barbara, Group V = transplants originating from Vredenberg, and group C = transplants originating from CARMABI.

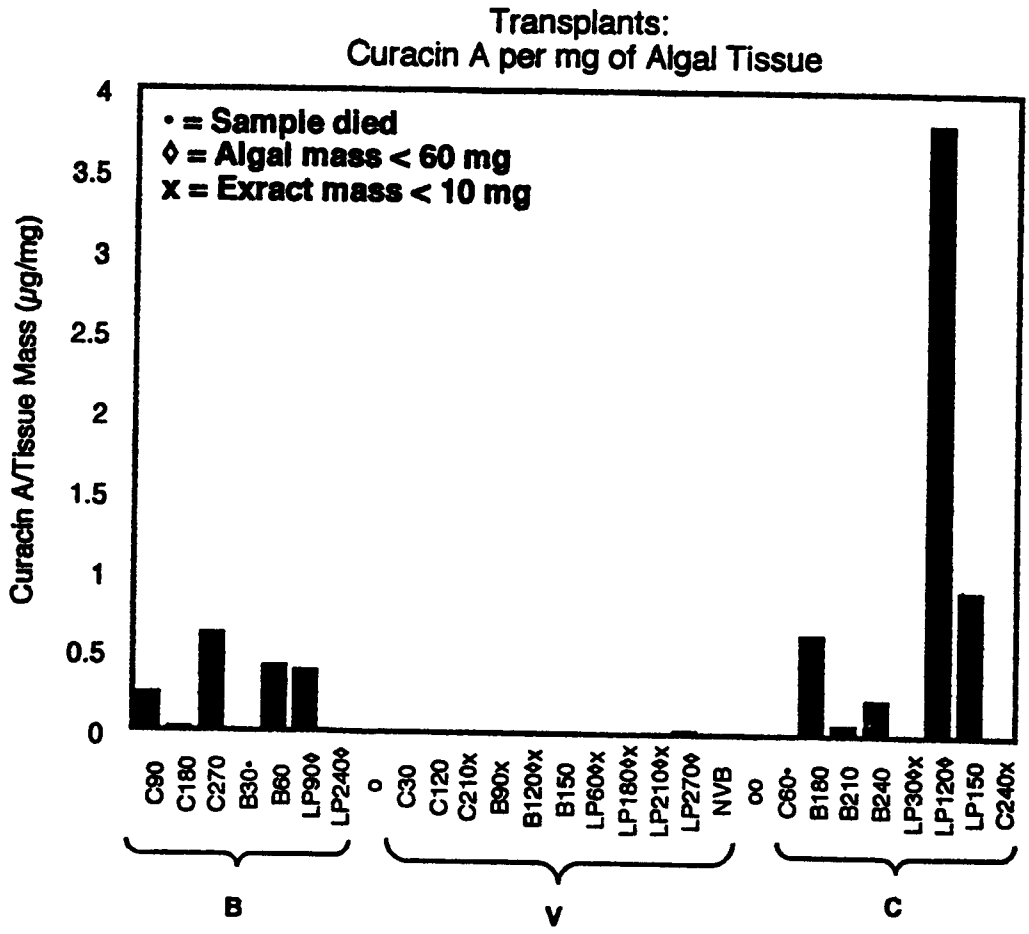

Figure 2.9 *L. majuscula* transplants: curacin A per unit of tissue mass Group B = transplants originating from Santa Barbara, Group V = transplants originating from Vredenberg, and group C = transplants originating from CARMABI.

This preliminary result points to a plausible genotypic difference in curacin A producing strains. Future directions may include a repeat of this field experiment over a longer duration coupled with the transplantation of a curacin A producing strain to a non-producing location. Elicitor studies aimed at inducing secondary metabolism in cultured strains of *L. majuscula* and other cyanobacterial species are currently being designed in our laboratory.

CHAPTER 3: BIOSYNTHESIS OF CURACIN A

Abstract

Feeding experiments using both radioisotope and stable isotope precursors have established that the lipid portion of curacin A originates entirely from acetate. Additions of methyl groups at C17 and methoxy positions were shown to derive from methionine. ^{13}C-NMR was used to assign the labeling pattern in curacin A from the supplied precursors. Mass spectral analysis of the molecular ion cluster together with integrated peak intensities from NMR spectra gave results which support the incorporations of the provided substrates; [1,2-^{13}C]-acetate, [1-^{13}C,^{18}O]-acetate and [Me-^{13}C]-methionine.

Introduction

Most biosynthetic studies on cyanobacteria to date have been directed toward primary metabolism including photorespiration, storage polymers and tetrapyrols.[29-31] Emanating from this research have been important findings such as the presence of an interrupted tricarboxylic acid cycle which lacks both succinyl CoA synthase and α-ketoglutarate dehydrogenase (figure 3.1).[32] This altered pathway seems to be present in most genera.[33] Another pathway involving both primary and secondary metabolism is the mode by which isopentenyl pyrophosphate (IPP) and dimethylallyl pyrophosphate (DMAPP) are produced. Recent evidence has accumulated for the presence of a nonmevalonate pathway to these compounds in some microorganisms including cyanobacteria.[34] While by no means complete, the evolving study of primary metabolism in cyanobacteria provides a background for the study of secondary metabolites.

Various collections of *L. majuscula* from tropical marine environments produce an impressive array of bioactive compounds. Some are chemically unique structures such as kalkitoxin (**1**), antillatoxin (**2**), lyngbya carbonate (**3**), and ypaoamide (**4**) (figure 3.2)

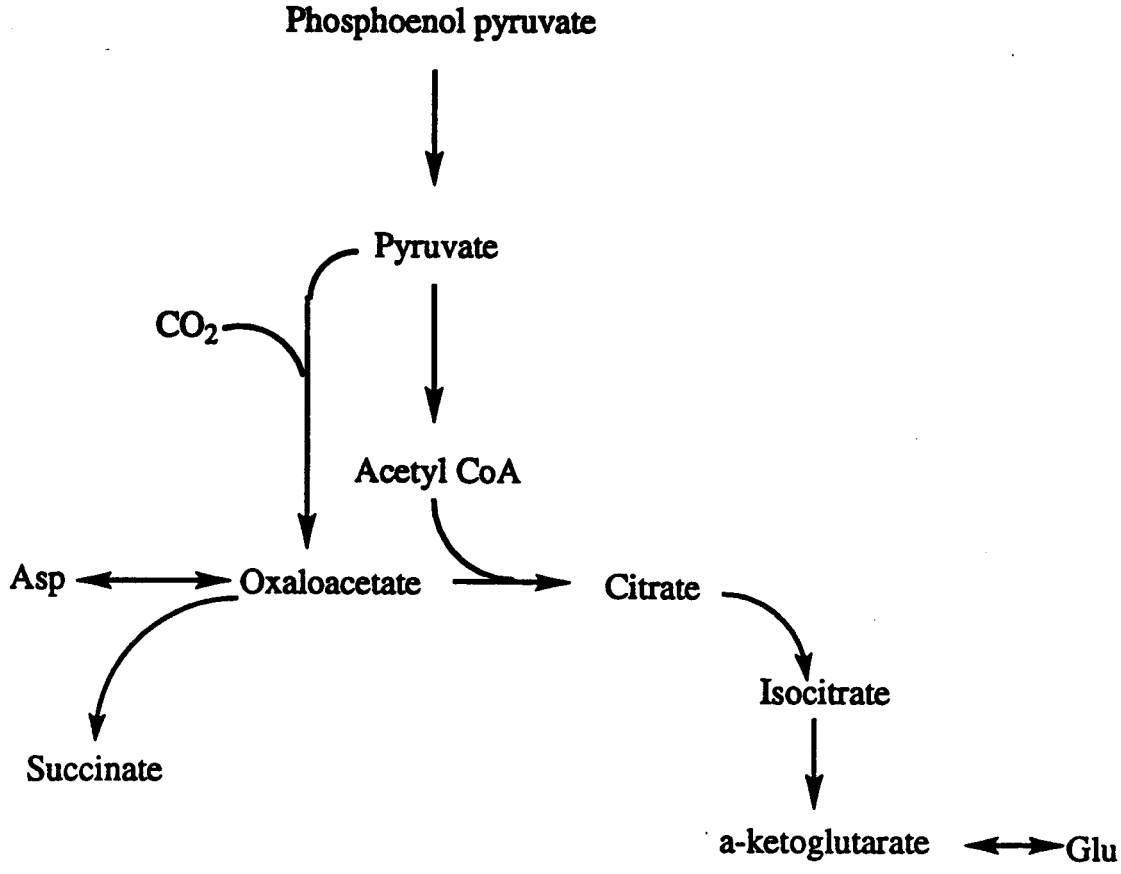

Figure 3.1 Schematic representation of the interuppted TCA cycle in some cyanobacteria

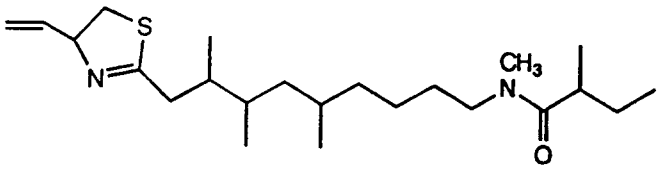

1

Kalkitoxin

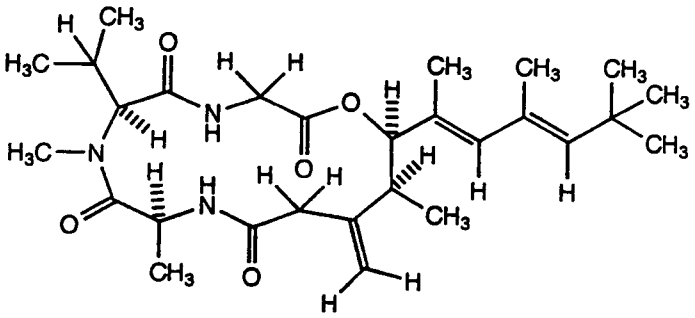

2

Antillatoxin

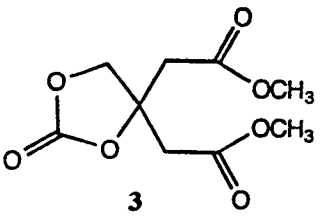

3

Lyngbya Carbonate

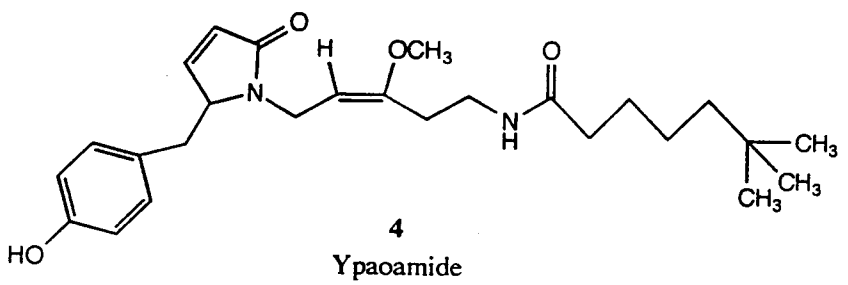

4

Ypaoamide

Figure 3.2 Unique bioactive metabolites from *L. majuscula*

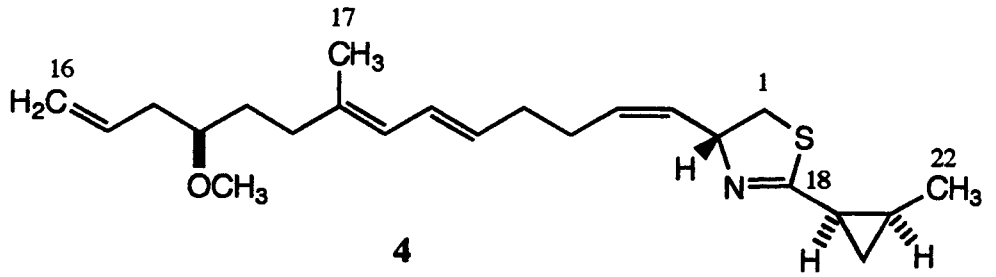

4

Curacin A

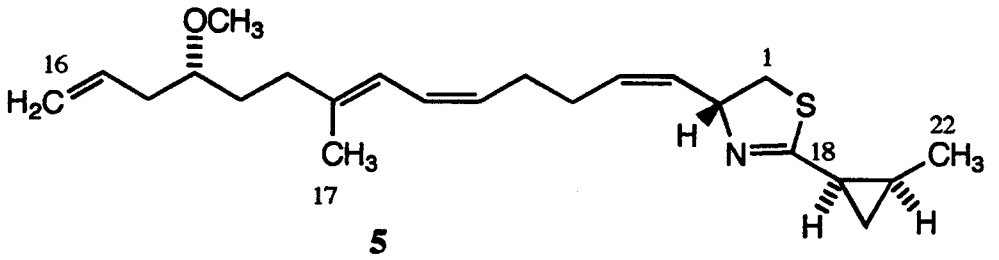

5

Curacin B

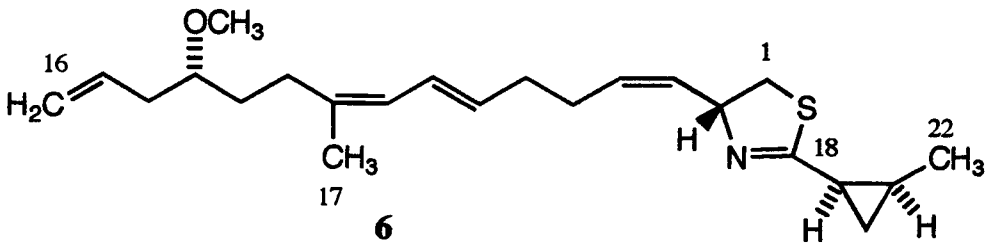

6

Curacin C

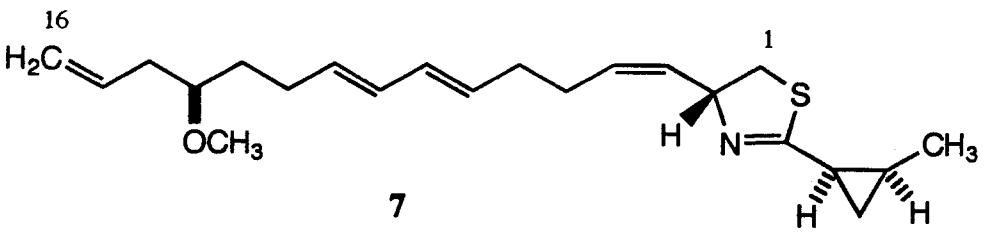

7

Curacin D

Figure 3.3 Structures of curacins A-D from *L. majuscula*

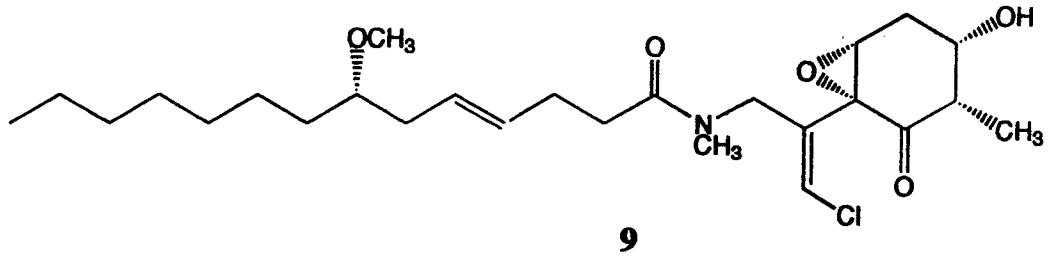

9

Malyngamide I

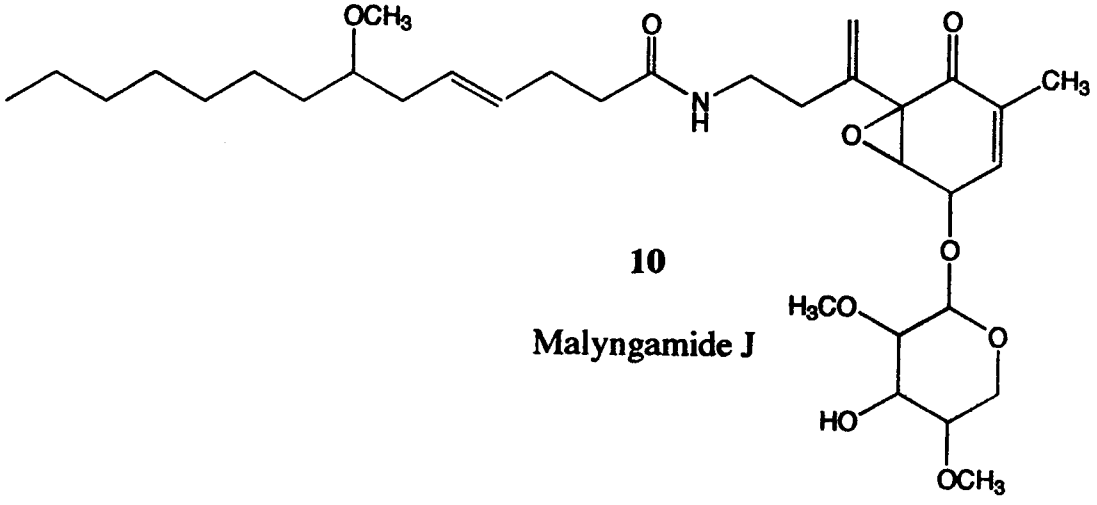

10

Malyngamide J

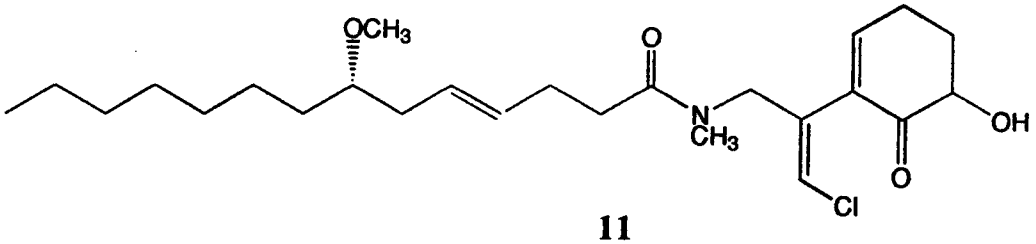

11

Malyngamide K

Figure 3.4 Structures of malyngamides I-K from *L. majuscula*

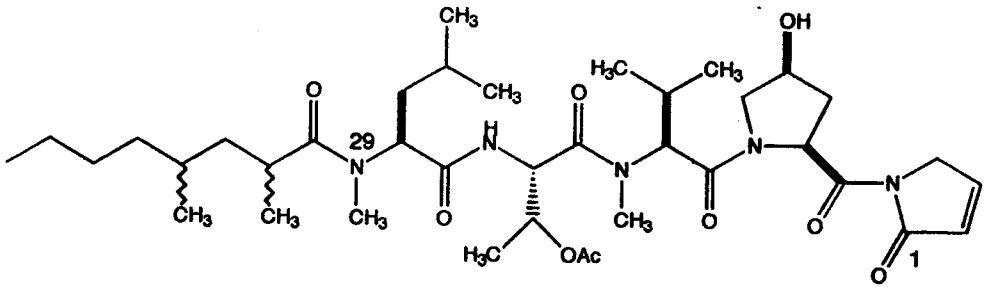

12

Microcolin A

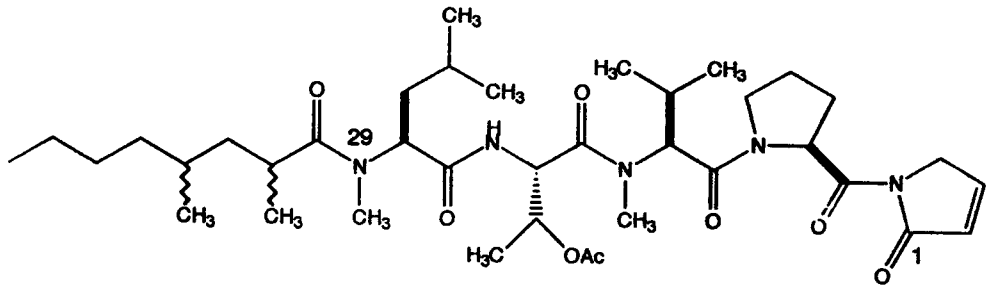

13

Microcolin B

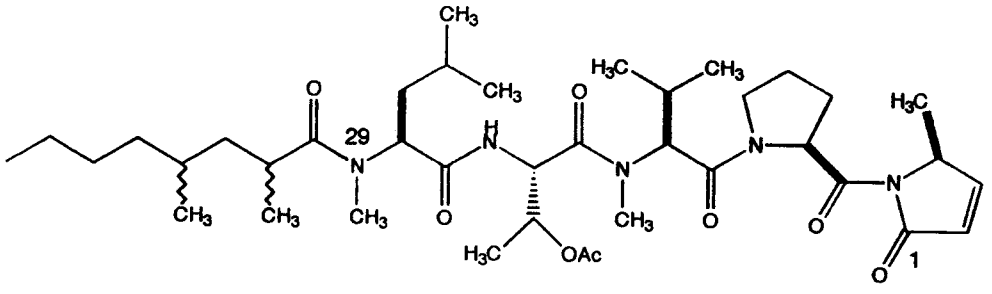

14

Microcolin C

Figure 3.5 Structures of microcolins A-C from *L. majuscula*

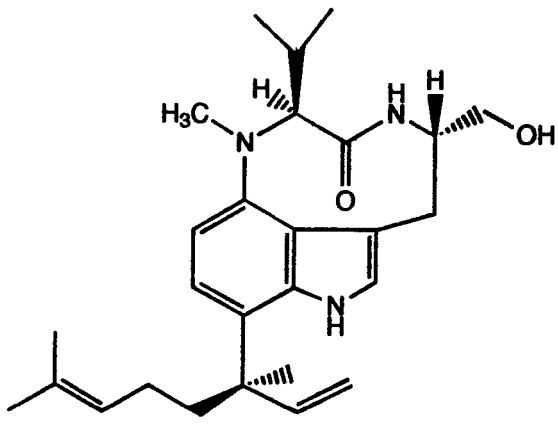

15

Lyngbyatoxin A

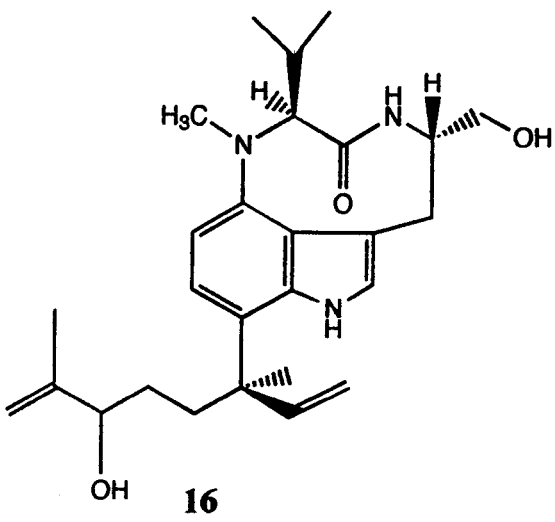

16

Lyngbyatoxin B

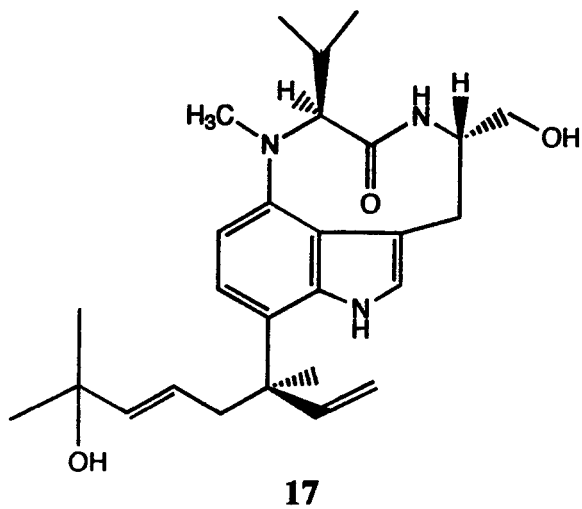

17

Lyngbyatoxin C

Figure 3.6 Structures of lyngbyatoxins from *L. majuscula*

where no naturally occurring analogs are known. Other *Lyngbya* metabolites occur in subclasses of structurally related compounds which most probably share at least one major common biogenic precursor. Examples of this are observed in curacins A-D[35,36] (**5-8**) (figure 3.3), the newly reported malyngamides I-K (**9-11**) (figure 3.4), microcolins A-C (**12-14**) (figure 3.5), and lyngbyatoxins A-C (**15-17**) (figure 3.6). Differences within these subclasses may be manifested as patterns of oxidation, methylation, double bond isomerization and group substituents. For example, the malygamides all contain a 14 or 16 member lipid region which possesses a 7-methoxy group. Modifications within the malygamide subclass surround this structural theme which is integrated into the fatty acid amide portion of these agents. Within the curacin subclass, curacin A (**5**) has the olefin configuration of 3Z, 7E, 9E, curacin B (**6**) has the configuration 3Z,7Z,9E, and curacin C (**7**) has the 3Z,7E,9Z configuration. Curacin D (**8**) is related to curacin A by the absence of the vinyl methyl group at C17.

Structurally, curacin A resembles a modified lipid with bicyclic functionalities composed of a thiazoline and a cyclopropyl ring. The combination of lipid character both with a nitrogen, sulfur heterocycle and a cyclopropyl moiety suggests a mixed biogenesis. In the proposal of such a scheme, the lipid portion is assembled through condensation of malonate and acetate as their coenzyme A thioesters with a concomitant release of CO_2. This is followed by reduction of the carbonyl groups with NADPH. Olefins are introduced by dehydration of the resulting hydroxl groups. The thiazoline ring is likely to be formed from the cyclization of cysteine plus one carbon from another amino acid. This latter unit may be contributed by a hydrophobic amino acid such as leucine or valine which additionally cyclizes to form the cyclopropyl ring. These amino acids may exist as a dipeptide prior to incorporation with the lipid portion of the curacin A skeleton. Alternatively the cyclopropyl group could originate from methyl addition to an olefin mediated by S-adenosyl methionine (SAM). This could occur by generation of the carbocation which would lead to cyclization with loss of H^+. A third possibility exists whereby the ring could result from the cyclization of DMAPP or IPP. In the latter case DMAPP or IPP may arise from either a mevalonate or a non-mevalonate pathway.

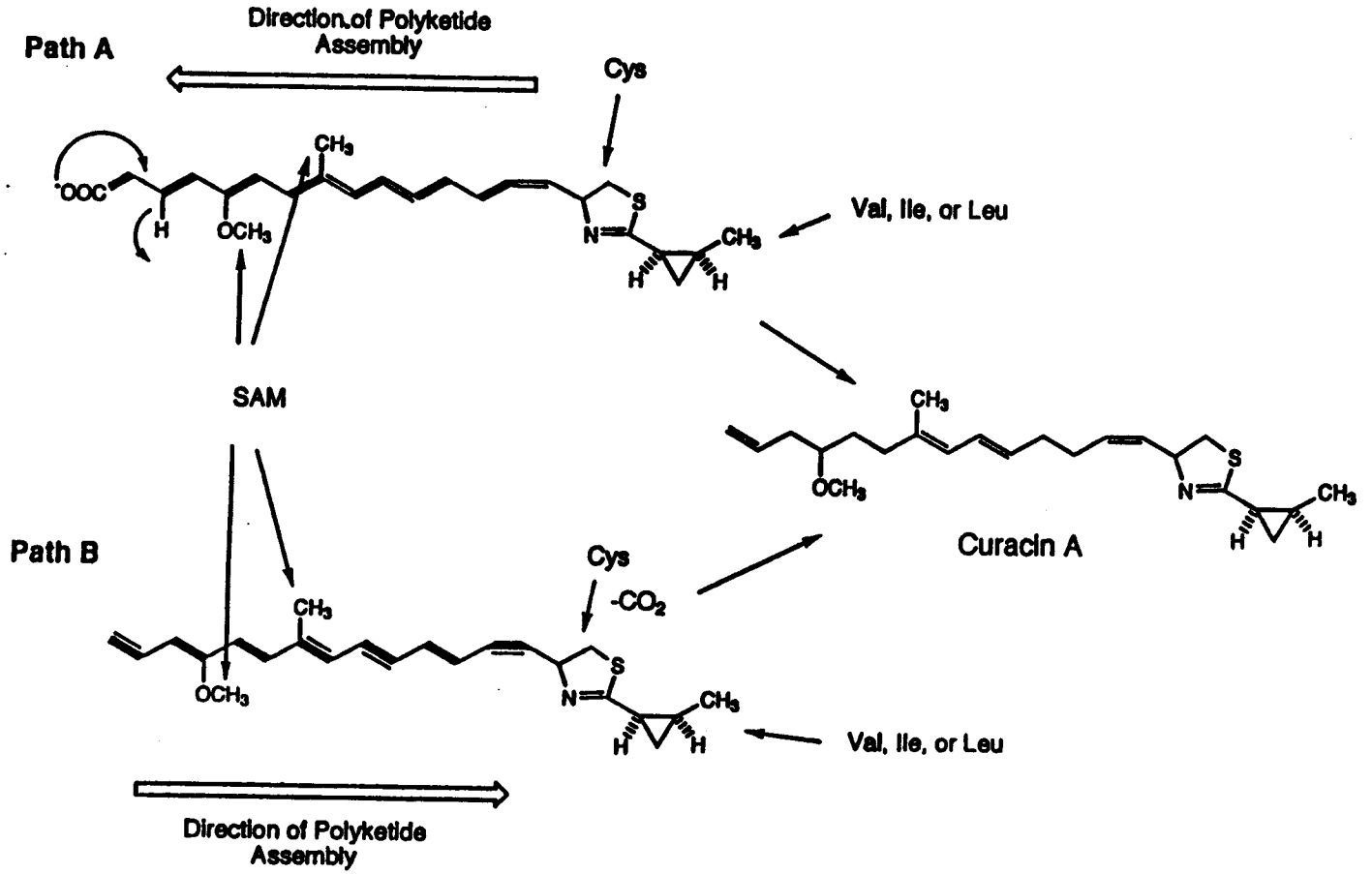

Figure 3.7 Two alternative biosynthetic pathways leading to curacin A

Direction of acetate assembly suggests whether cysteine (or a cysteine containing dipeptide) is condensed with the preformed chain or whether the polyketide assembly process is cysteine-initiated. These two alternative pathways are depicted in figure 3.7. Methylations at the C-13 methoxy and C-10 methyl group are likely to arise from methionine via SAM.

Cultures of *L. majuscula* maintained in our laboratory produce both curacin A and barbamide. Characterization of these cultures with respect to the timing of curacin A production, described in the previous chapter, has been used to guide the following biosynthetic experiments. A combination of radioisotope and stable isotope feedings were used to monitor integration of a precursor into the target structures. ^{13}C NMR and GC-EIMS were used to evaluate enrichment of ^{13}C labeled precursors into curacin A. Insights from these experiments regarding the pathway leading to barbamide will be discussed in chapter 4.

Experimental Methods

^{14}C, ^{3}H, and ^{35}S precursor feedings: Radiolabeled precursors were supplied to two or three day old cultures. Substrates fed were; [1-^{14}C]-acetate, [2-^{3}H]-acetate, [^{35}S]-L-cysteine, [U-^{14}C]-L-leucine, [U-^{14}C]-L-valine, [3,4,5-^{3}H]-L-leucine, and [Me-^{14}C]-L-methionine. Inocula were approximately 100 mg of tissue added to 1 L flasks containing 250 mL SWBG11. Each labeling experiment was run in duplicate. After 10 days incubation the tissue was harvested, blotted dry, weighed, and extracted in 2:1 MeOH:CH_2Cl_2. Attempts to generate a high specific activity metabolite with [1-^{14}C]-acetate or [2-^{3}H]-acetate made use of variable incubation durations (9-13 days) and pulse feeding schedules (2-3 feedings per incubation period). The media was assayed at time of label introduction by adding a 100 or 500 μL (depending on μCi fed) aliquot of the medium to a liquid scintillation cocktail (LSC) (Aquascint) in duplicate and counting the sample (Beckman LS 6000).

[^{35}S]-L-cysteine was prepared as a stock solution in sterile H_2O at a concentration of 250 μCi/mL. Two 1L cultures of *L. majuscula* were equilibrated for 2 days and 10 μCi of the labeled material were fed to each flask. Incubation lasted ten days after which tissue was harvested and extracted.

A small aliquot (5-10 μL) from each crude radiolabeled preparation was chromatographed by 2D TLC on aluminum back silica plates. Developing solvents were 10% MeOH/$CHCl_3$ in the first dimension and 50% EtOAc/hexanes in the second. The chromatograms were then evaluated by TLC linear analysis with radioisotope detection (Berthold Tracemaster 20).

Sep-Pak fractionation was performed on all samples as previously stated which was followed by normal phase HPLC (μ-porosil) with UV detection using 4% EtOAc:hexanes as the mobile phase. The curacin A peak eluting at 19.8 min was collected, solvent was reduced *in vacuo*, and the compound was resuspended in 1.0 mL of hexanes. Ten microliters of this sample was evaluated in duplicate by LSC. Specific activity was determined by twice assaying a 1/100 dilution of the stock solution by UV spectrophotometry at λ = 242 nm (Hewlett Packard Model 8452 A diode array UV-VIS spectrophotometer).

^{13}C labeled precursor feedings: All isotopes were purchased from Cambridge Isotope Laboratories and were 98% enriched in ^{13}C. [1-^{18}O,^{13}C]-acetate was a generous gift from Dr. Steven Gould. Stable isotope feedings were initiated by feeding [U-^{13}C]-acetate to 10 X 3 L Fernbach flasks containing three day old cultures of *L. majuscula* each in 1 L of SWBG11 medium. All cultures were placed in a culture room at 28°C and provided with uniform illumination. A total of 160 mg of label was incubated with the cultures for 10 days. Tissue was harvested and extracted in 2:1 CH_2Cl_2:MeOH as before with the exception that the Sep-Pak fractionation in EtOAC:hexanes was replaced by a larger scale silica column fractionation (15 cm X 1.5 cm). Normal phase HPLC purification gave 21.2 mg of curacin A. The HPLC pure curacin A was evaluated for overall enrichment by GC-EIMS. One dimensional ^{13}C NMR and 2D INADEQUATE experiments were run in C_6D_6 at 100 MHz. Percent enrichment in ^{13}C from [U-^{13}C]-acetate labeling of curacin A was

calculated from the following equation:

Equation 3.1

$$\frac{(I_S - I_W)(100)}{I_T} = \text{Percent } ^{13}C \text{ enrichment from [U-}^{13}C\text{]-acetate}$$

The variables I_S and I_W represent the integrals for the strong and weak intensity doublets observed for each signal respectively. I_T is the total integration at that center. Percent enrichment reflects the amount of the total ^{13}C at a given site that participates in an intact unit coupling.

The origin of the methoxy oxygen in curacin A was determined by supplying 5 X 1 L cultures of *L. majuscula* with 135 mg [1-^{13}C,^{18}O]-acetate on day 2 after inoculation. On day 4 another 135 mg of labeled substrate was added. Tissue harvest and extraction was performed on day 7. Chromatography was done as stated above. HPLC gave 11.2 mg of curacin A. A ^{13}C NMR spectrum was recorded at 100 MHz in C_6D_6.

[CH_3-^{13}C]-L-methionine (150 mg) was supplied to 5 X 1.5 L cultures after 2 days of equilibration to investigate the methylation pattern at C17 and OCH_3. The incubation period lasted 9 days after which the tissue was harvested, extracted and processed as before.

Study of the role of L-leucine as a possible precursor to curacin A was investigated by feeding a total of 500 mg [2-^{13}C]-L-leucine to 5 X 1.5 L cultures of *L. majuscula* on day 3 after inoculation. After a 10 day incubation period, the cultures were harvested, extracted, and processed as before.

Results and Discussion

^{14}C and ^{35}S precursor feedings: Four independent experiments were performed using radiolabeled acetate. These tests explored the effect of varying the label introduction time, duration of incubation, and feeding protocols. Incorporation of [1-^{14}C]-acetate was 1.7%

in the best of the series. This incorporation justified feeding the [U-^{13}C] substrate on a larger scale for the determination of exact enrichment levels. In a later experiment aimed at biosynthetically generating a high specific activity probe for kinetic binding studies with tubulin, an incorporation of 4.05% was reached. [^{35}S]-L-cysteine was also taken up by *L. majuscula* to form the thiazoline of curacin A and the thiazole of barbamide at low yet significant levels (see table 1). Methionine labeled with ^{14}C on the methyl group was also incorporated into both natural products. Culture performance was compromised in the presence of both cysteine and methionine which likely accounts for low precursor uptake. Dithiothreitol is commercially added to [^{35}S]-L-cysteine as a sulfur reductant. This was later found to be toxic to the cultures. The cause of culture instability resulting from methionine feeding is unknown. Two dimensional TLC linear analysis with radioisotope detection did, however, show both cysteine and methionine to significantly label curacin A.

Cyclization of either valine or leucine was proposed in the formation of the cyclopropyl group of curacin A. Both of these amino acids were incorporated into the structure with a higher level of incorporation resulting from the leucine feeding. Data showing amount fed, incorporation levels, and specific activity from radioisotope precursor feedings are listed in Table 3.1.

Radiolabeled L-leucine was supplied in another experiment where [3,4,5-^{3}H]-L-leu was co-administered with [U-^{14}C]-L-leu. This incubation resulted in an isotope discrimination favoring ^{14}C incorporation. The ^{3}H to ^{14}C ratio in the isolated curacin A was 7.4 times less than that in the media at the start of the experiment. This extreme isotope discrimination suggests that more than one transformation is taking place prior to incorporation. In fact both the anabolic and catabolic paths leading to and from L-leucine formation involve precursors which may be even more suitable as a cyclopropyl forming compound than leucine itself. For example, α-ketoisokaproate can be formed from leucine via transaminase action. The keto center then renders the methylene protons more susceptible to abstraction which would precede cyclization. Another possibility involves the catabolism of leucine leading to HMG-CoA which is a precursor to mevalonate.[38] If *L. majuscula* possesses the mevalonate pathway to IPP/DMAPP, this route could explain

indirect incorporation of the hydrophobic amino acids. A third possibility is that the amino acids were catabolized to acetate before incorporation into curacin A.

Precursor	Amount fed μCi	δ_{SA} prec. mCi/mmol	†Curacin A produced μg	Curacin % incorp.	Curacin A δ_{SA} dpm/pmol
[1-^{14}C]-acetate	4.83	54.00	285.00	1.40	0.15
[1-^{14}C]-acetate	5.08	54.00	311.00	1.70	0.19
[1-^{14}C]-acetate	7.00	54.00	-	1.68	-
[1-^{14}C]-acetate	66.20	54.00	2362.69	4.05	0.93
[2-^{3}H]-acetate	3500	16 Ci/mmol	-	-	0.28
[^{35}S]-L-cys	16.80	600Ci/mmol	190.97	0.13	0.06
[U-^{14}C]-L-val	14.39	250	1540.00	0.95	0.07
[U-^{14}C]-L-leu	17.42	292	2340.00	1.86	0.11
*[U-^{14}C]-L-leu + *[3,4,5-^{3}H]-L-leu	5.3 6.7	292 120 Ci/mmol	- -	2.2 0.31	- -
[CH$_3$-^{14}C]-L-Met	14.95	54.00	-	0.11	-

Table 3.1 Radiolabled precursors fed to cultures of *Lyngbya majuscula*.
* Values are average of two isotope discrimination cofeeding experiments.
† Mass determined by UV at λ_{max} = 242, ε = 28,000 M^{-1} cm^{-1}.

Stable isotope precursor feedings: [1,2-^{13}C]-acetate labeled curacin A was analyzed by GC-EIMS. The molecular ion cluster of labeled compound showed additional M+1 and M+2 intensity when compared to an unlabeled sample. In addition, M+3 and M+4 signals were observed which were not detected in the unenriched spectrum. Figure 3.8 shows a comparison of ion abundances which have been normalized to m/z = 373. Analysis of the molecular ion cluster showed considerable enrichment in the labeled curacin A. From this data, 2.1% of the total carbon of the isolated curacin A was labeled with ^{13}C accumulated from the incorporation of catabolized and intact [1,2-^{13}C]-acetate.

Carbon 13 NMR was used in three modes to detect enrichment in curacin A. First, intact incorporation of a uniformly labeled ^{13}C substrate was detected by observing spin-spin coupling of carbon nuclei that are adjacent to each other. Second, singly labeled substrates, such as ^{13}CH$_3$-methionine, were evaluated for their ability to enrich carbons in comparison with unlabeled centers. Third, ^{18}O enrichment was detected by measuring the upfield shift of the methoxy bearing carbon from [1-^{18}O]-acetate feedings.

Both 1D carbon and 2D INADEQUATE ^{13}C NMR spectra were recorded for the [U-^{13}C]-acetate enriched curacin A at a field strength of 100 MHz. INADEQUATE spectra allowed carbon-carbon connections to be assigned. Figures 3.9 and 3.10 show the 1D and 2D experiment respectively. Horizontal lines in the 2D spectrum indicate intact

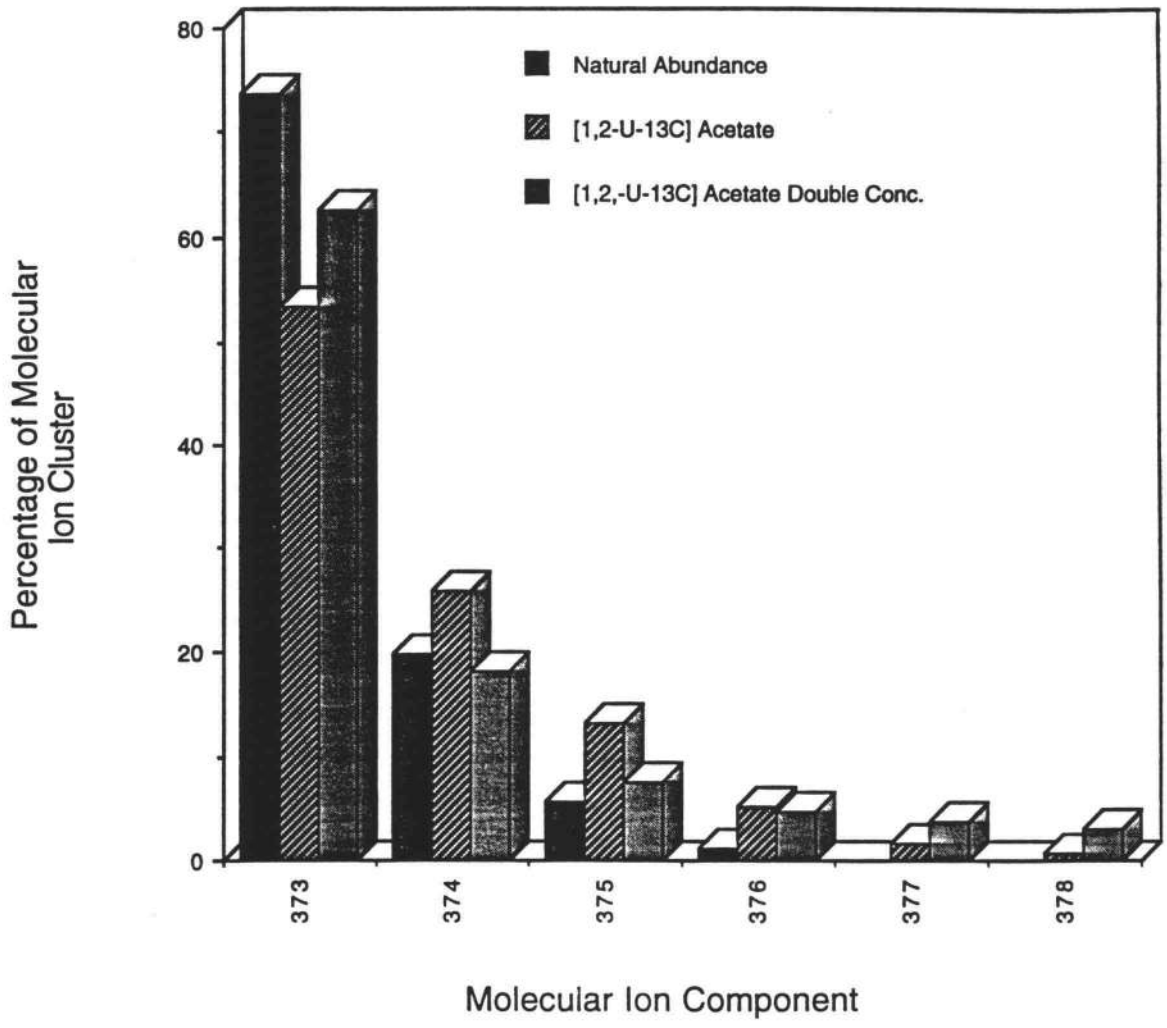

Figure 3.8 Analysis of molecular ion cluster by GC-EIMS for [1,2-^{13}C]-acetate labeled curacin A. Integrals of of ions were taken and summation from m/z = 373-378 reflect 100% of ion cluster for each experiment.

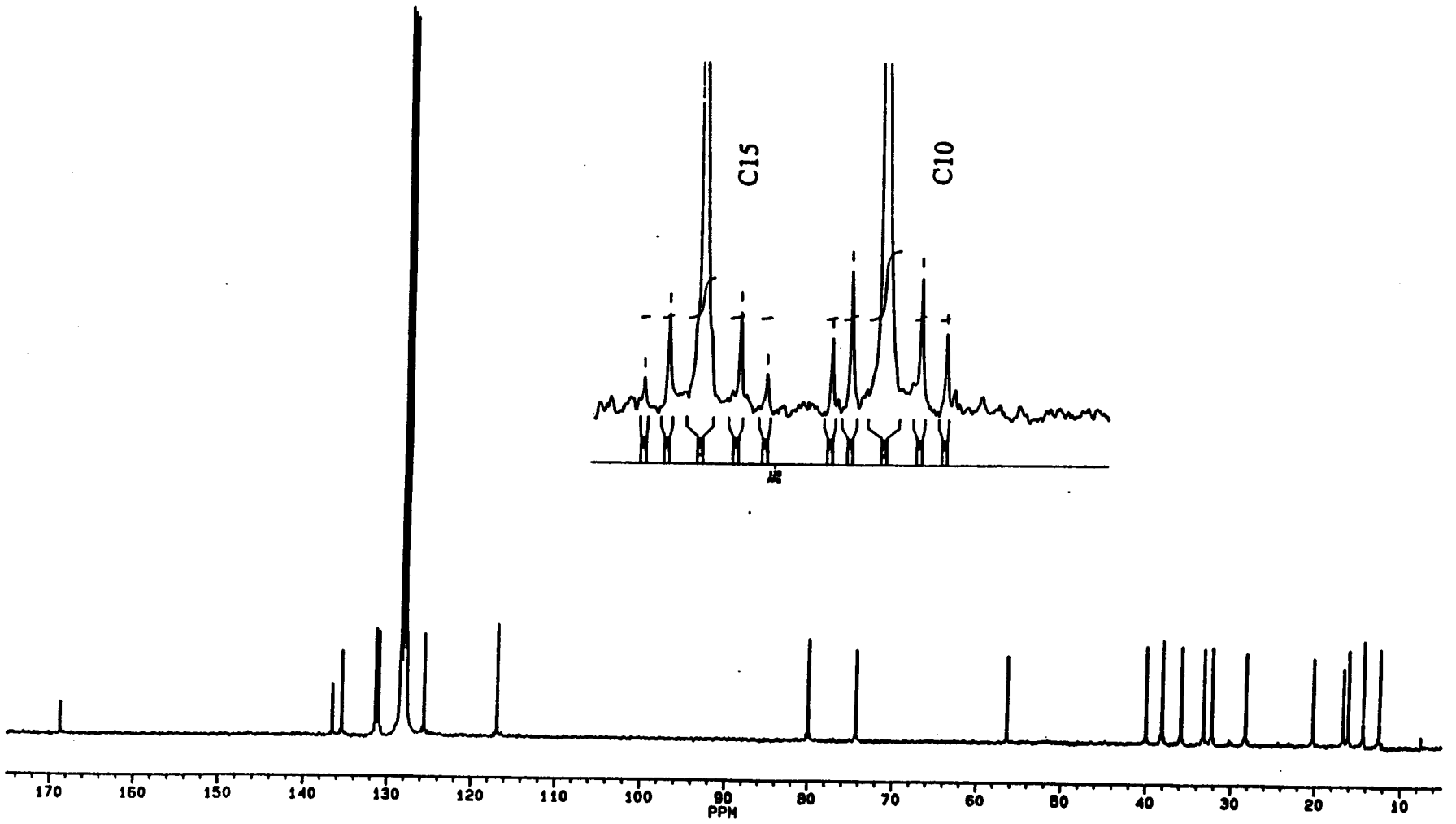

Figure 3.9 1D ^{13}C NMR spectrum of [1,2-^{13}C]-acetate labeled curacin A expansion of signals from C15 and C10 show details of coupling pattern observed for most signals.

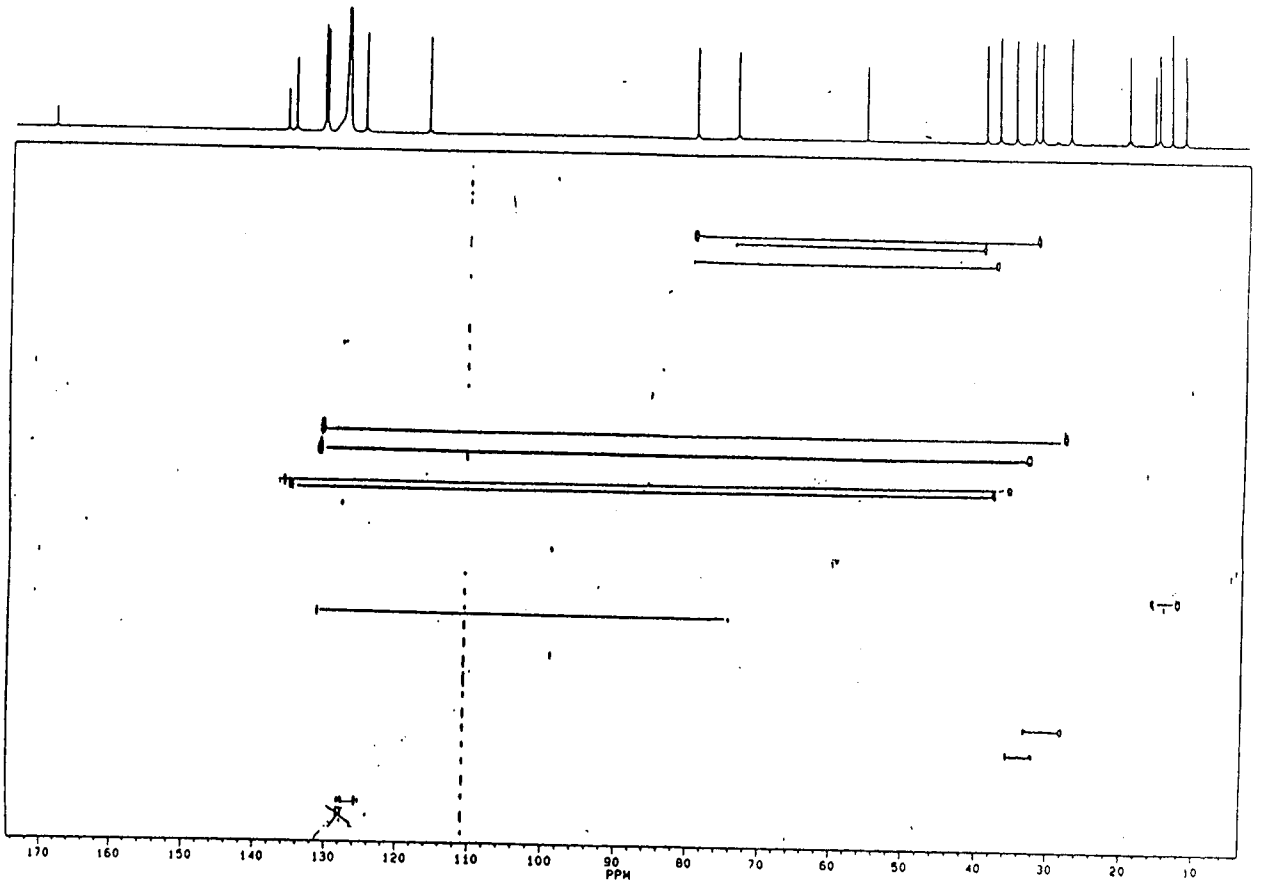

Figure 3.10 2D INADEQUATE Spectrum of [1,2-^{13}C]-acetate labeled curacin A

bond incorporations. All carbon atoms in the compound were shown to be enriched by the uniformly labeled acetate indicating extensive metabolism of the provided substrate. This resulted in elevated concentrations of ^{13}C in endogenous metabolic pools. From analysis of the signals showing intact ^{13}C incorporation, percent enrichment (eg. the percentage of total ^{13}C) was calculated for each center. Carbon signals C1-C15 and C19-C22 in the ^{13}C NMR spectrum showed a complex coupling pattern of at least two sets of doublets, not found in the natural abundance spectra, which flanked the centerline peaks. Each of the two sets of doublets for a given signal between C4-C16 were clearly of different intensities. For each signal, the lesser intensity doublet was interpreted to result from coupling of an adjacent nonuniformly labeled unit, likely resulting from the extensive metabolism of the intact, uniformly labeled acetate ($^{13}CH_3$-$^{13}COO^-$) to a singly ^{13}C labeled precursor ($^{13}CH_3$-$^{12}COO^-$ or $^{12}CH_3$-$^{13}COO^-$). By examination, a pattern emerged which was consistent with the superposition of intact bond enrichment upon a background of unintact label enrichment. The greater intensity coupling represents the sum of intact unit incorporation plus the statistical probability of $^{13}CH_3$-$^{13}COO^-$ enrichment following metabolism and reassembly of the substrate. Total ^{13}C at a carbon center was calculated by summing the integrated intensity for each doublet and the centerline peak. Intact unit incorporation was determined by calculating the difference between the integrated intensities of the two sets of doublets with respect to the total ^{13}C present. This was converted to percent enrichment by factoring in 100. Percent enrichments in ^{13}C are summarized in table 3.2. Determination of intact incorporation was calculated (see experimental equation 3.1). The doublets of some signals overlapped thus obscuring analysis for some carbon positions.

C#	δ ppm	J Hz (strong)	J Hz(weak)	% inner set	% outer set	% total ^{13}C enrichment
1	39.92	29.8		6.0	-	
2	74.29	48.4	29.4	4.8	5.1	0.3
3	131.2	48.2	30.1			
4	130.9	42.5	42.0	11.1	a	-
5	28.16	42.2	33.5	4.7	9.5	4.8
6	33.12	44.1	33.4	5.5	11.1	5.6
7	131.35	44.0	88.8	9.4	a	-
8	127.89	51.0	83.4	7.0	0.5	6.5
9	125.53	64.6	73.5	9.6	3.8	5.8
10	136.43	43.0	73.3	12.4	8.4	4.0
11	35.79	42.9	38.1	4.3	8.7	4.4
12	32.10	39.3	38.0	6.4	12.9	6.5
13	79.97	39.3	obs	14.7	a	-
14	38.05	42.6	38.2	5.0	8.3	3.3
15	135.34	42.7	69.5	10.8	5.3	5.5
16	116.77	69.3		7.8		

Table 3.2 Coupling and enrichments of carbon centers in curacin A as determined by ^{13}C nmr. % Inner set and % outer set refer to the ^{13}C signals visible as doublets either closest to or farther from the centerline signal respectively.

In addition to establishing acetate as the precursor for the lipid portion of curacin A, the direction of polyketide assembly was also apparent. Coupling constants (J) were assigned to either strong or weak intensity doublets. As these were compared, coupling partners became identifiable. For instance, the larger intensity coupling constants for C14 and C15 were 42.6 Hz and 42.7 Hz, respectively, and could be recognized as an intact unit. A pattern consistent with cysteine-initiated chain assembly was therefore observed corresponding to path A in figure 3.7.

Attempts to increase intact incorporation by cofeeding labeled acetate with unlabeled citrate were unsuccessful. The purpose of supplying citrate was to flood the TCA cycle with an intermediate downstream from acetate. This was done with the hope that unintact incorporation would be minimized. A shorter duration feeding in the presence of a higher media concentration of [1,2-^{13}C]-acetate was also performed but resulted in higher unintact incorporation, again stemming from extensive metabolism of the substrate.

Three possibilities exist for the origin of the methoxy oxygen of curacin A. It could derive from the acetate oxygen at C-1, by O_2 addition to the polyketide chain, perhaps by a cytochrome P450 mediated event, or by H_2O addition. Cultures that were administered [1-^{13}C,^{18}O]-acetate yielded curacin A, which by ^{13}C-NMR showed the oxygen bearing carbon (C-13), to be labeled by ^{18}O. This was apparent from the upfield shifted component of the signal at δ = 79.97 ppm. Integration of this signal revealed that 30.8% of the ^{13}C at that center carried an ^{18}O. A section of the spectrum showing this signal is depicted in figure 3.11. The shifted component was broadened and gave $\Delta\delta$ = 0.02 ppm, which is consistent with previously reported values for ^{18}O shifted carbon signals.[37] This result shows convincingly that the methoxy oxygen originated from acetate through polyketide assembly. It also clearly identifies C1 of this acetate unit, and hence, the likely path for acetate assembly.

Curacin A posseses two or possibly three sites that could be methlyated by methionine via SAM. These centers are located at the methoxy group, the vinyl methyl, and C-20, the cyclopropyl methylene. Cultures supplied with [Me-^{13}C]-methionine died back upon introduction of the label. This was followed by a stabilization period where the cultures took up the ^{13}C labeled substrate.

The ^{13}C-NMR spectrum of the isolated curacin A from this feeding experiment showed the methoxy peak at δ = 56.3 ppm and C-17 at δ = 16.58 ppm to be selectively enriched over natural abundance. No enrichment was observed for C-20, consistent with the original prediction that the cyclopropyl group is derived from a hydrophobic side chain amino acid or DMAPP/IPP. The ratio of signal intensity from carbons that were labeled to those that were unenriched was calculated. These ratios were compared to corresponding ratios calculated from the natural abundance spectrum. Specific enrichment of C-17, the vinyl methyl was 2.33 % (eg. 2.12 times larger than natural abundance) and enrichment for the methoxy methyl group was 2.50 %. Figures 3.12a and 3.12b show the ^{13}C-NMR spectrum of the methionine enriched sample and natural abundance spectrum, respectively.

The feeding of [2-^{13}C]-L-leucine was expected to label position C18 of curacin A. This is a quaternary center in the thiazoline ring. However, careful assessment of the ^{13}C-

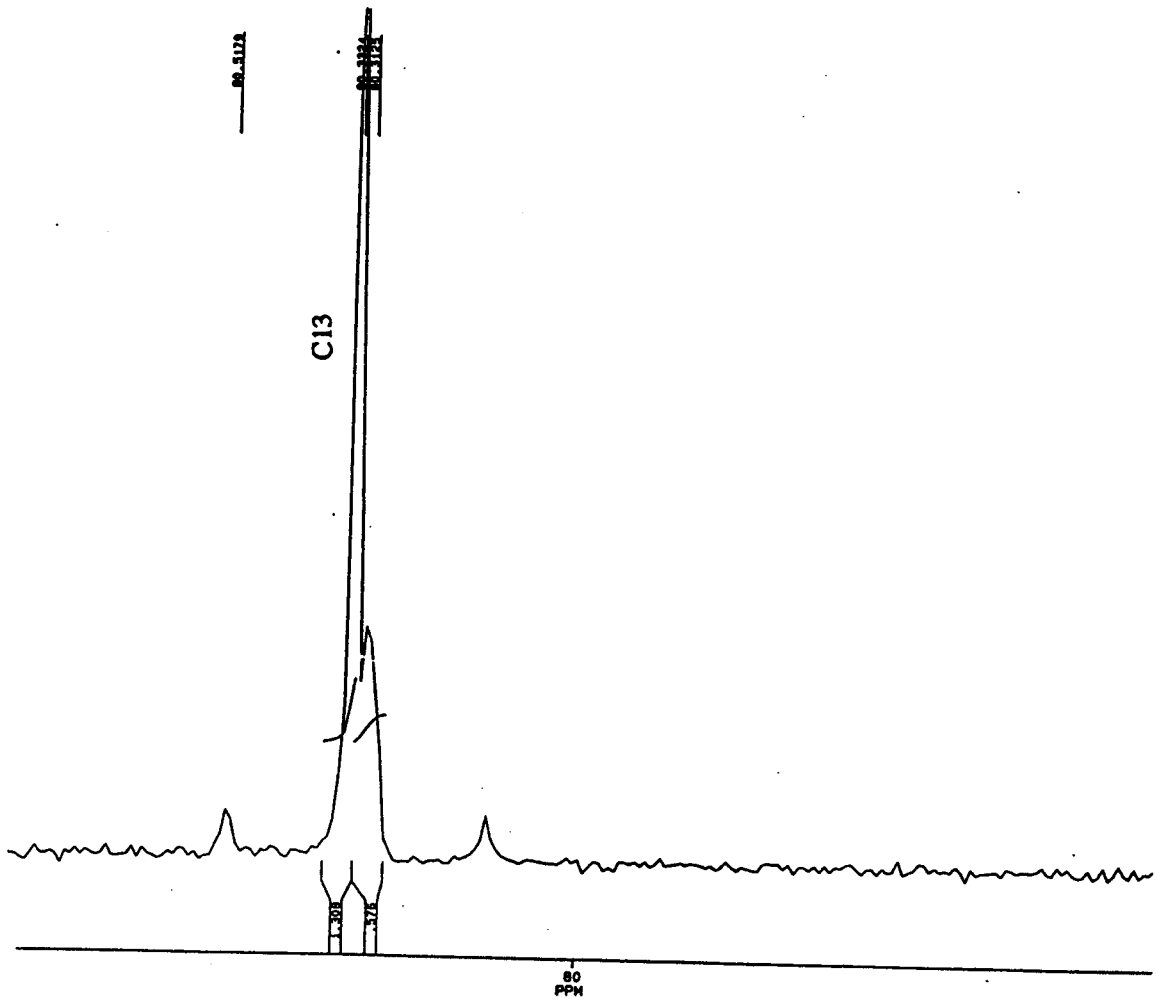

Figure 3.11 ^{13}C NMR Peak of [1-^{13}C,^{18}O]-acetate labeled curacin A showing upfield component of the carbon 13 signal due to ^{18}O enrichment. Satellite signals are due to natural abundance coupling to the ^{13}C labeled center.

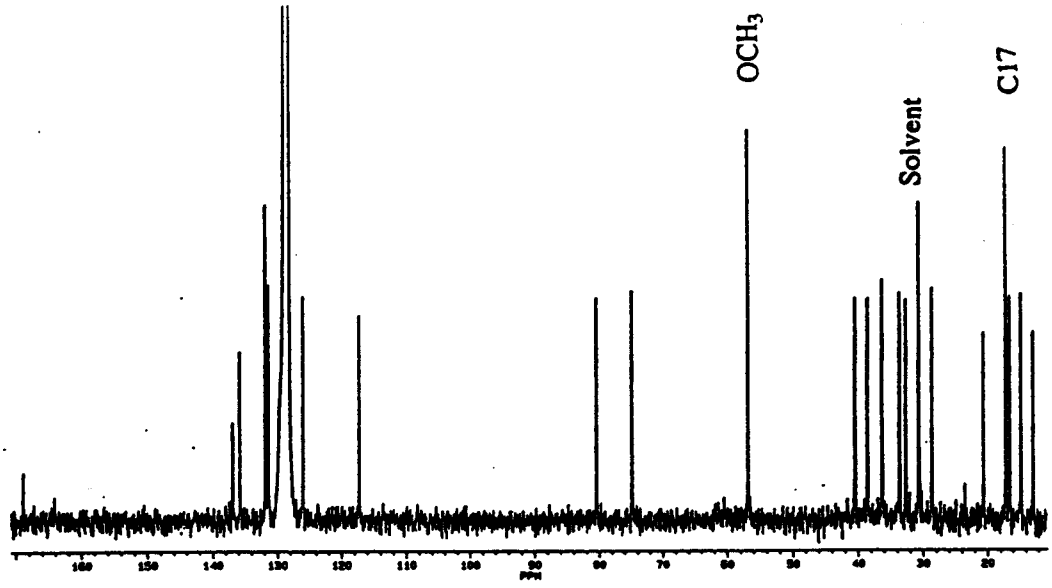

Figure 3.12a ^{13}C NMR spectrum of [methyl-^{13}C]-methionine enriched curacin A

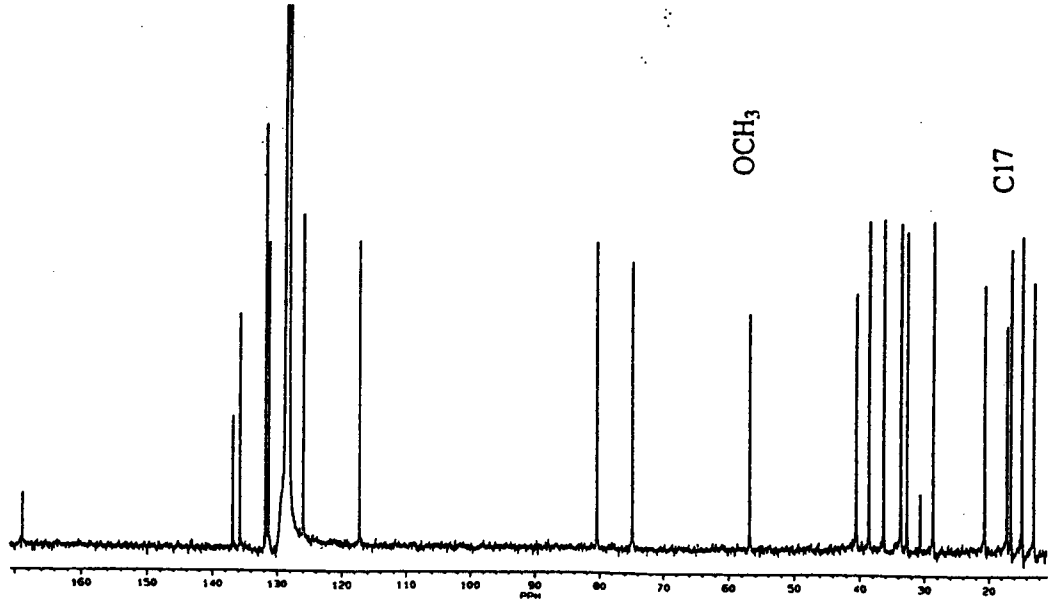

Figure 3.12b ^{13}C NMR spectrum of natural abundance curacin A

NMR spectrum showed no enrichment in ^{13}C. This was in apparent contradiction to our findings from the ^{14}C labeled amino acid feedings. This finding suggests that incorporations from these earlier studies resulted from metabolic breakdown of the substrate before incorporation into curacin A in a nonspecific manner.

The failure of L-leucine to label the metabolite indicates that the precursor to the cyclopropyl group may be DMAPP/IPP. Feedings with mevalonate have often resulted in low incorporations either due to low uptake or invocation of a nonmevalonate pathway, found to be present in some cyanobacteria.[34] If IPP or DMAPP were established as precursors, their origin from the mevalonate or nonmevalonate pathways could be distinguished from feeding [1-^{13}C]-acetate.

In conclusion, this series of precursor studies has revealed the acetogenic nature of the polyketide portion of the molecule including the oxygen center and the likely direction of assembly. Methylation of this oxygen at C13 and origin of the C17 vinyl methyl group were both found to originate from L-methionine. This supports our biosynthetic proposal that these entities are introduced by a SAM mediated event. Incorporation of ^{35}S from cysteine is preliminary evidence that the thiazoline ring originates from this amino acid. Confirmation of this result may be provided by future [U-^{13}C]-L-cys or [^{15}N]-L-cys feedings.

The scheme in figure 3.13 reflects our findings in the context of a standard polyketide pathway. Assembly of the hexaketide portion is initiated by the condensation of an enzyme bound cysteine with malonyl ACP (derived from acetate and CO_2). Five additional Claisen-type condensations are envisioned to take place to form the remainder of the chain. Double bond formation, while not proven, is likely to take place during the assembly of the carbon skeleton whereas methylation probably takes place after assembly.

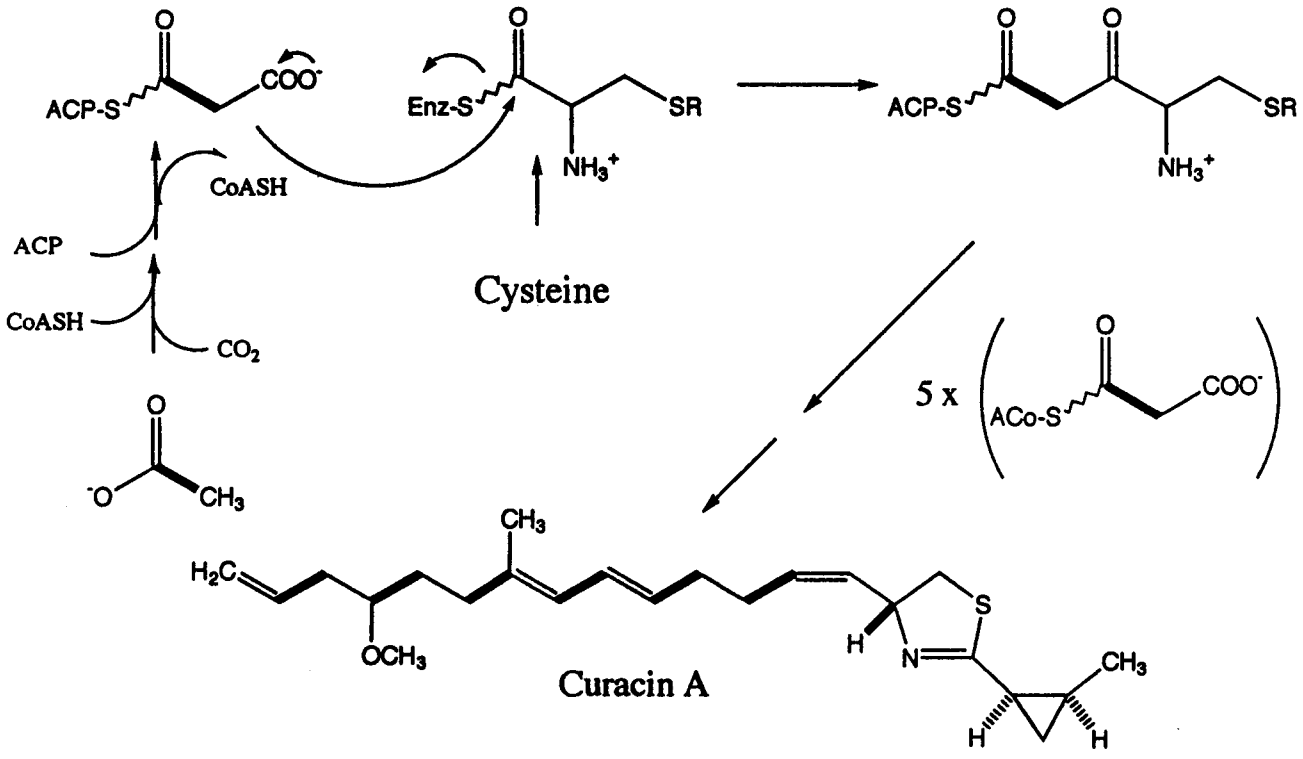

Figure 3.13 Scheme for cysteine-initiated polyketide assembly leading to curacin A

CHAPTER 4

INSIGHTS INTO THE BIOSYNTHESIS OF BARBAMIDE

Abstract

Precursor feeding studies on cultures of *L. majuscula* that produce the molluscicidal agent, barbamide, have shown the trichlorinated portion of the molecule to derive from L-leucine. ^{13}C Enrichment of the compound was confirmed through the use of ^{13}C-NMR and FAB-MS. Double labeled [1-^{13}C,^{18}O]-acetate was taken up by the alga, as determined by curacin A labeling, but was not incorporated into the barbamide skeleton.

Introduction

Fractionation of an extract derived from a Curaçao collection of *Lyngbya majuscula* led to the isolation of several biologically active metabolites. Among them were the brine shrimp toxic compound curacin A, and the ichthyotoxic compounds malygamide H (**1**) and antillatoxin (**2**) ($LD_{50} < 25$ mg/mL).[40] From a fraction determined to possess molluscicidal activity, the trichlorinated compound barbamide (**3**) was isolated. The compound was toxic to the freshwater snail *Biomphalaria glabrata* at a level of ($LD_{50} < 10.0$ μg/mL). *Biomphalaria glabrata* is the host of a larval stage of the parasitic blood fluke *Schitozoma sp.* which has been shown to induce chronic anemia and organ infections in regions of Africa and South America.

Barbamide (**3**) consists of a phenyl and a thiazole ring which are bridged by a methylene and a methine carbon which is linked to an N-methyl amide moiety. Extending from the amide is a branched hydrocarbon tail which bears an unusual trichloromethyl functionality.

Several isolates of *L. majuscula,* which were brought back to the lab for subculture, produced both curacin A and barbamide while some only produced curacin A.

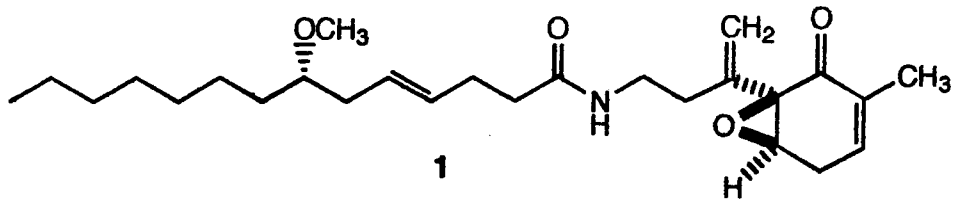

1

Malyngamde H

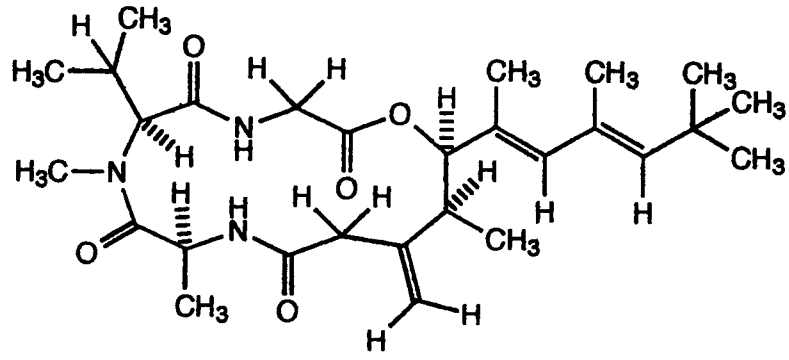

2

Antillatoxin

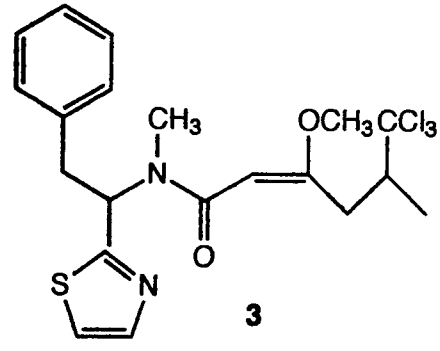

3

Barbamide

Figure 4.1 Bioactive metabolites from a field collected strain of *Lyngbya majuscula*

One of the curacin A and barbamide subcultured strains performed well upon initial screening for desirable growth characteristics and was therefore selected for pathway studies. Because both metabolites shared some of the same metabolic precursors in their proposed pathways (figures 3.7 and 4.3), we hoped to gain knowledge about barbamide metabolism at the same time as we studied the curacin A biosynthesis.

The presence of halogens in structures of marine origin, especially bromine, illustrates one of the interesting differences between marine and terrestrial metabolites.[41] Halogens, which are abundant in the marine environment, are utilized by a variety of marine bacteria, cyanobacteria, and invertebrate species for the biosynthesis of chlorinated and brominated metabolites with possible chemical communicative or chemoprotective roles.

The compounds dysidin (**4**), dysidenin (**5**), and a diketopiperazine derivative (**6**) originally isolated from the sponge *Dysidea herbacea* each possess trichloromethyl groups.[42] Cyanobacterial filaments have been shown to be present as a symbiont with this sponge species. In 1993 researchers isolated cell types from both the sponge and the symbiont. Mass spectral and NMR analysis were performed on the cell extracts to determine which organisms produce **4**, **5**, and **6**. Using the trichloromethyl group as a chemical signature of these compounds by mass spectrometry, the identity of the producer of these polychlorinated structures was ascribed to the cyanobacterial symbiont.[43]

The branched structure that bears the trichloromethyl group in barbamide and in the *Dysidea*/cyanobacterial metabolites, are postulated to arise from the L-leucine side chain. Our original proposed biosynthetic scheme for barbamide included the amino acids phenylalanine and cysteine as precursors to the phenyl and the thiazole ring respectively. Completion of the thiazole ring likely requires inclusion of the carboxyl group from phenylalanine. L-leucine is condensed to a two carbon unit and was thought to be chlorinated at an early stage during leucine biosynthesis. A likely scenario for this would be the addition of Cl^+ to pyruvate. The two ring system is associated with the two carbon unit which was thought to derive from acetate. Figure 4.3 details the earlier proposed pathway. Methlyation at the amide nitrogen and the olefinic oxygen are thought to derive from methionine via SAM.

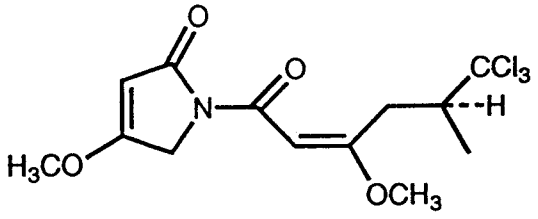

4

Dysidin

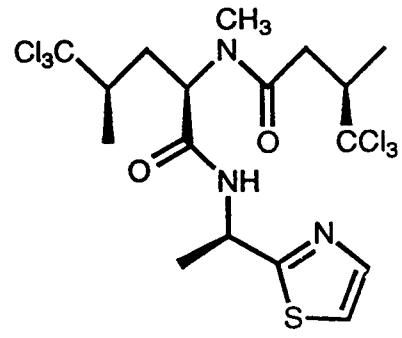

5

Dysidenin

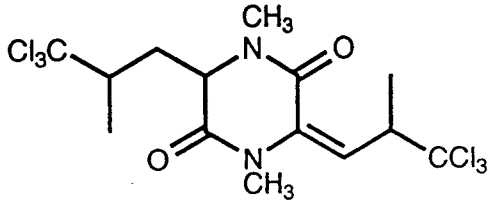

6

Figure 4.2 Sponge/cyanobacteria metabolites that contain trichloromethyl groups

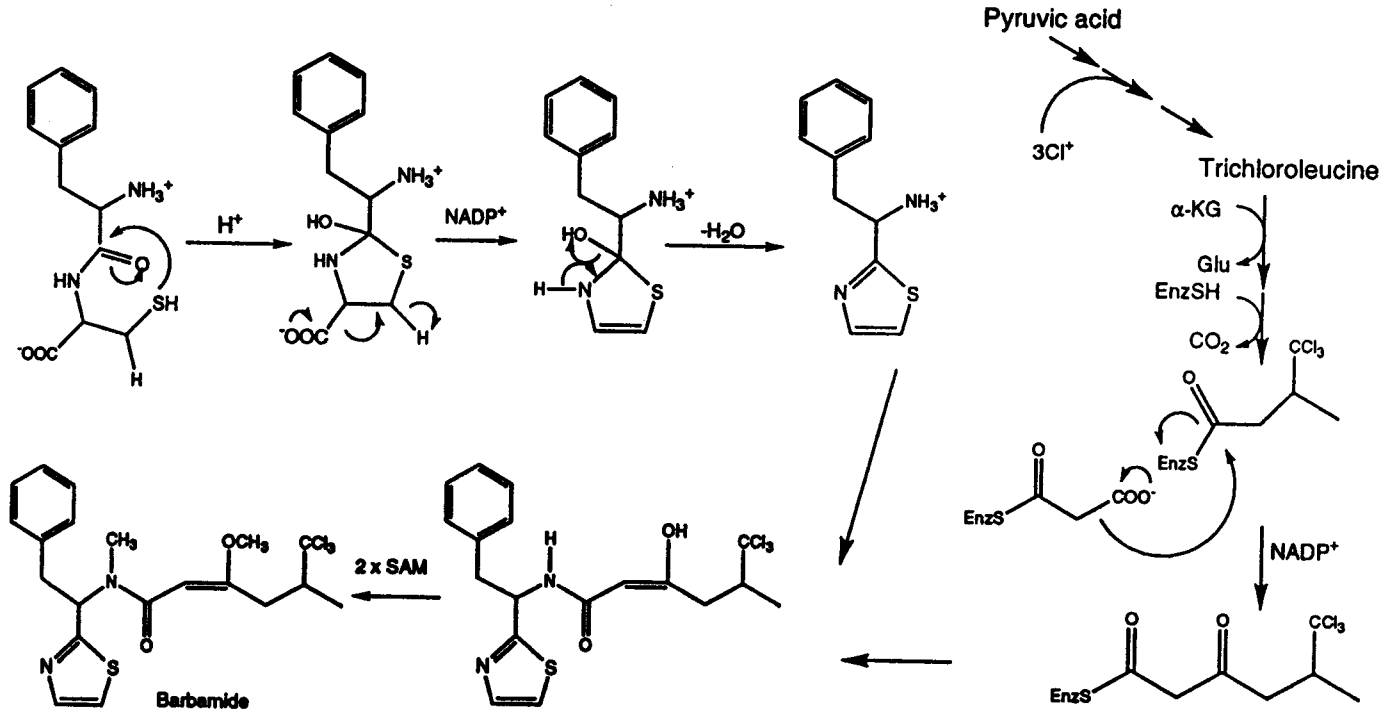

Figure 4.3 Original proposed biosynthesis of barbamide from primary precursors

Several of the feedings described in Chapter 3 produced extracts which upon fractionation yielded labeled barbamide. Samples were prepared for ^{13}C-NMR and MS analysis and evaluated in a similar fashion to curacin A.

Experimental

Radiolabeled precursors: Culture conditions and feeding of the precursors [^{35}S]-L-cys, [U-^{14}C] acetate, [U-^{14}C]-L-leu, and [U-^{14}C]-L-valine were carried out as described in chapter 3. Sep-Pak fractionation in 50% EtOAc/hexanes yielded a green pigmented solution containing barbamide. HPLC of this fraction in 40% EtOAc/hexanes (μ-porosil) gave pure barbamide. Two dimensional TLC analysis of the crude extract and LSC of the medium and purified compounds were carried out as previously described.
Stable isotope precursors: Quantities of [^{13}C-Me]-L-methionine, [1-^{13}C,^{18}O]-acetate, [1,2-^{13}C]-acetate, and [2-^{13}C]-L-leucine were supplied to two or three day old cultures of *L. majuscula* as described in Chapter 3. Silica flash chromatography using 50% EtOAc/hexanes as the mobile phase yielded the barbamide containing fraction. ^{13}C-enriched barbamide was further purified by normal phase HPLC with 40% EtOAc/hexanes as the eluent. 13C-NMR spectra were run at 100 Mhz in d_6-DMSO. FAB-MS were recorded on a Kratos MS50TC mass spectrometer. Ion clusters (m/z = 461.2-467.3) of the enriched and unenriched FAB-MS spectra were compared and graphically analyzed (Kaleidagraph) to show ^{13}C incorporation levels (figure 4.4).

Results and Discussion

Radioisotope feedings: Radiolabeled barbamide was evaluated by LSC and 2D TLC for incorporation of acetate, L-cys, L-val, and L-Leu. All of the substrates administered to the alga were incorporated. Levels of incorporation were roughly one half of that observed for curacin A when observed by TLC with radioisotope detection. Similar to

the result for curacin A, barbamide showed a preference for the branched amino acid L-leu over L-val. The thiazole precursor, L-cys, was taken up by the alga. Incorporation was low due to poor culture performance, however TLC and LSC analysis showed barbamide to be labeled by the precursor. The substrates that were administered to the cultures and their incorporation relative to total media radioactivity at the time of label introduction are summarized in Table 4.1.

Precursor	Amount fed μCi	δ_{SA} prec. mCi/mmol	Barbamide % incorp.
[1-^{14}C]-acetate	7.00	54.00	1.25
[^{35}S]-L-cys	16.80	600Ci/mmol	0.03
[U-^{14}C]-L-val	14.39	250	0.09
[U-^{14}C]-L-leu	17.42	292	0.41
[CH_3-^{14}C]-L-Met	14.95	54.00	

Table 4.1 Radiolabeled precursors supplied to *L. majuscula* and incorporated into barbamide.

Stable isotope feedings: HPLC pure barbamide from the [U-^{13}C]-acetate experiment was analyzed by ^{13}C-NMR. Extensive coupling of equal intensity was observed in all carbon signals indicating a lack of specificity in incorporation. Signals assigned to C5 and C6 (the expected site of incorporation) were not enriched to a significant extent over other carbons in the molecule. Another feeding of acetate in the form of [1-^{13}C,^{18}O]-acetate also failed to show specific enrichment. Analysis of the ^{13}C NMR spectrum for this feeding showed no enhancement of signals from oxygen bearing carbons which was in agreement with the [U-^{13}C]- acetate feeding result. Although this same feeding had yielded labeled curacin A, neither C6 (amide carbon) nor C4 (methoxy bearing site) showed the diagnostic upfield shifted component of the carbon signal. Taken together these results would suggest that acetate is not a direct precursor for the C5, C6 unit; however this negative result cannot entirely rule out the possibility of acetate as a precursor.

Observation of the N-Me and O-Me signals by ^{13}C-NMR after the [^{13}C-Me]-methionine feeding showed only slight enrichment over natural abundance and is not statistically significant. The same feeding gave convincing results for the methylation of

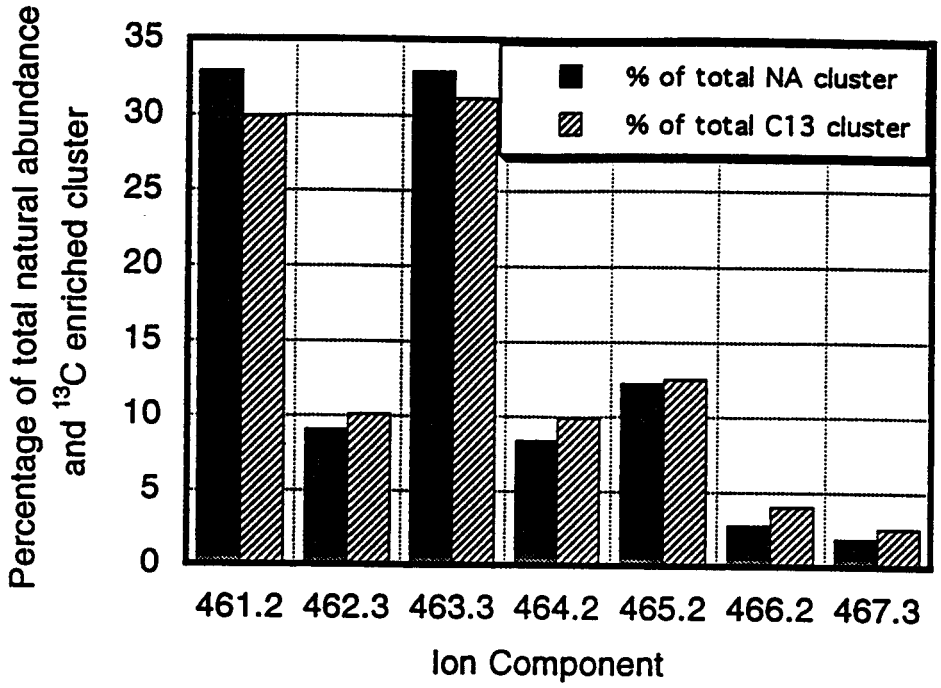

Figure 4.4 Analysis of FAB-MS ion cluster from [2-^{13}C]-L-leucine enriched barbamide compared to natural abundance (NA) spectrum. Summation of integrals from ions m/z = 461.2-467.3 account for 100% of total ion cluster from each spectrum.

curacin A, however because barbamide is usually labeled to a lesser extent than curacin A there exists the possibility that the substrate was in too limited supply.

Although [2-^{13}C]-L-leucine had failed to label curacin A, analysis of the isolated barbamide from this preparation showed an increased signal intensity at δ = 166.8 ppm, an unexpected site of labeling (figure 4.5). This center was assigned in the original structure determination work to the amide carbonyl; however upon close scrutiny of the complex region in the original HMBC spectra (figure 4.6), correlations were found from the methoxy protons at δ = 3.6 ppm to 166.8 ppm and from N-Me protons at δ = 2.88 ppm with the carbon at δ = 167.0 ppm. This observation requires that the assignments be modified from the original values[40] to place the methoxy bearing carbon C6 at δ = 167.0 ppm and the carbonyl C4 at δ = 166.8 ppm.

The enriched site C4 derives from the α carbon of L-leucine and showed an average specific enrichment of 4.11%. Figure 4.7 depicts the signal intensity of several natural abundance signals within the same spectrum as compared to the enriched signal at δ = 166.8 ppm. FAB-MS showed the M+1 ion signals to be increased proportionally to a decrease in natural abundance molecular ions by 4.4%. In other words 4.4% of the total barbamide isolated from the leucine feeding carried a ^{13}C label. Graphical comparison of natural abundance and ^{13}C enriched barbamide mass spectral data are shown in figure 4.4. The alternative possibility was that an analog of barbamide could have been generated by the feeding of excess quantities of L-leucine. Analysis of ^{1}H NMR, ^{13}C NMR and FAB-MS spectra revealed no evidence of the unchlorinated geminal dimethyl which would correspond to the side chain of leucine.

The result from the feeding of [2-^{13}C]-L-leucine, has guided us to modify our original proposal. Addition of Cl^{+} to an easily activated substrate such as pyruvate, a leucine biosynthetic intermediate, seems unlikely in that the [2-^{13}C]-L-leucine would have been extensively metabolized before it was incorporated into barbamide. The timing of chlorination is therefore different from our original proposal. Chlorination may take place via chlorine radical addition to the substrate rather than chloronium ion addition. The updated proposed pathway leading to barbamide is detailed in figure 4.8.

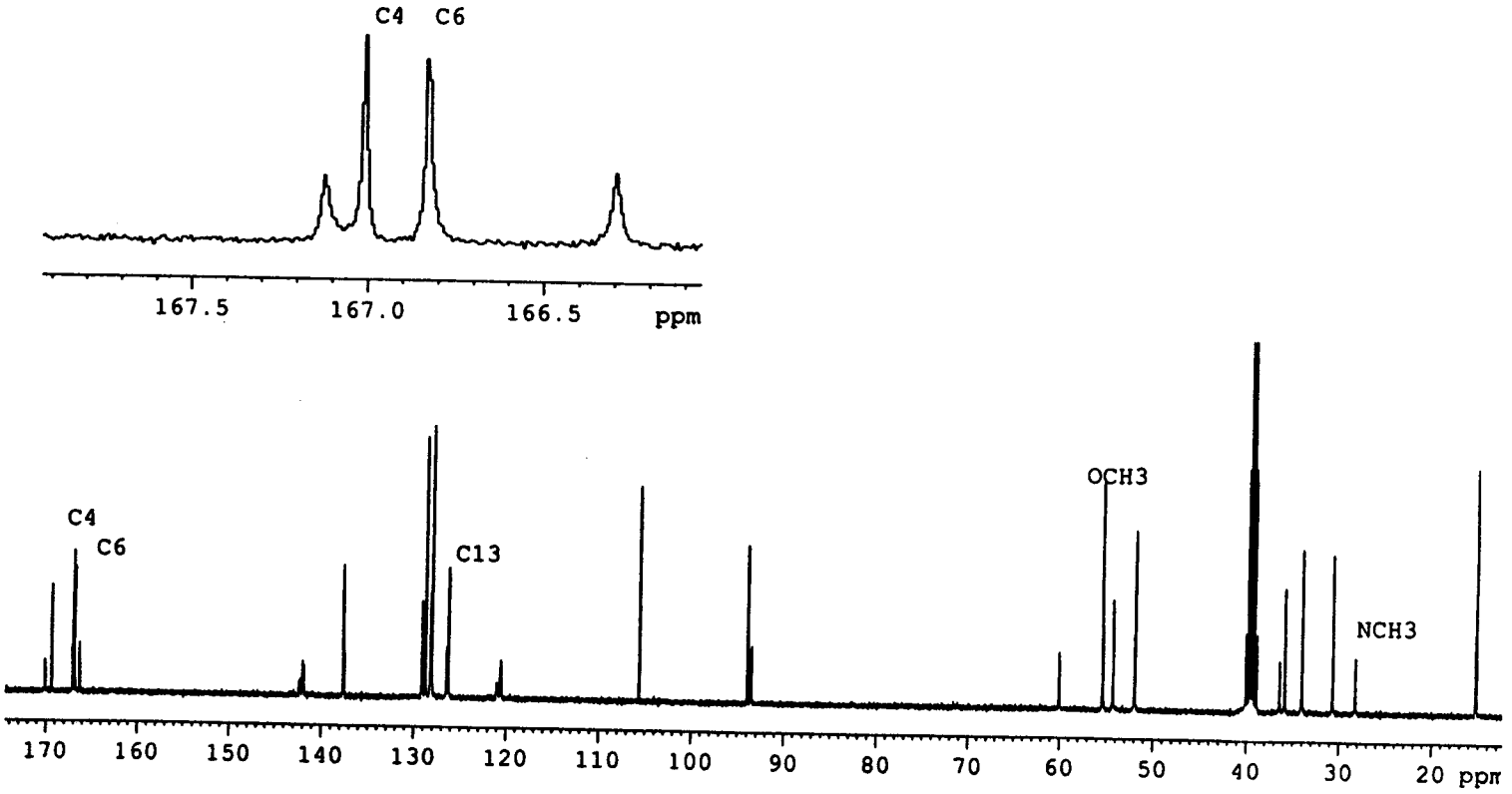

Figure 4.5a Natural abundance ^{13}C-NMR spectrum of barbamide

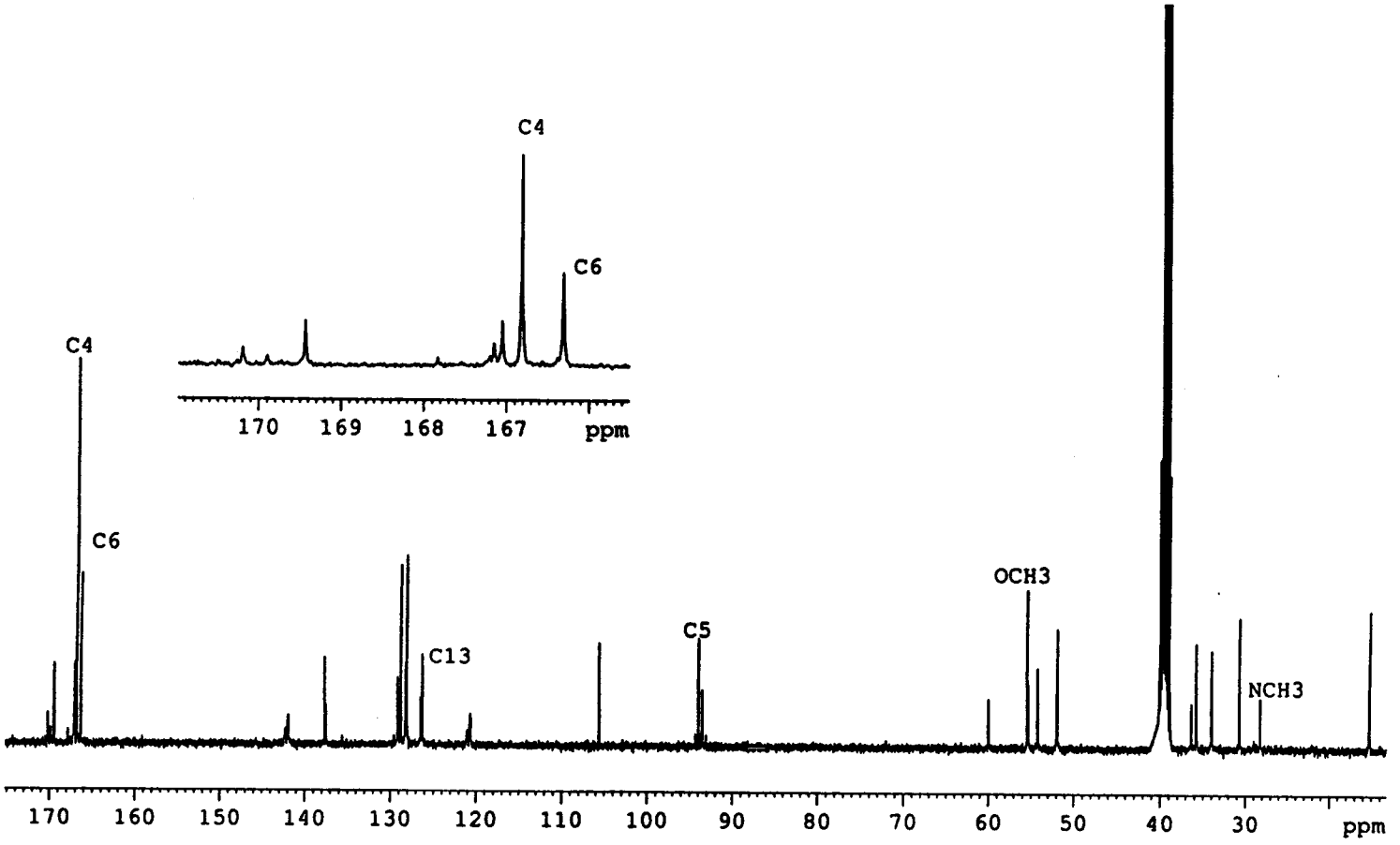

Figure 4.5b ^{13}C-NMR of [2-^{13}C]-L-leucine enriched barbamide

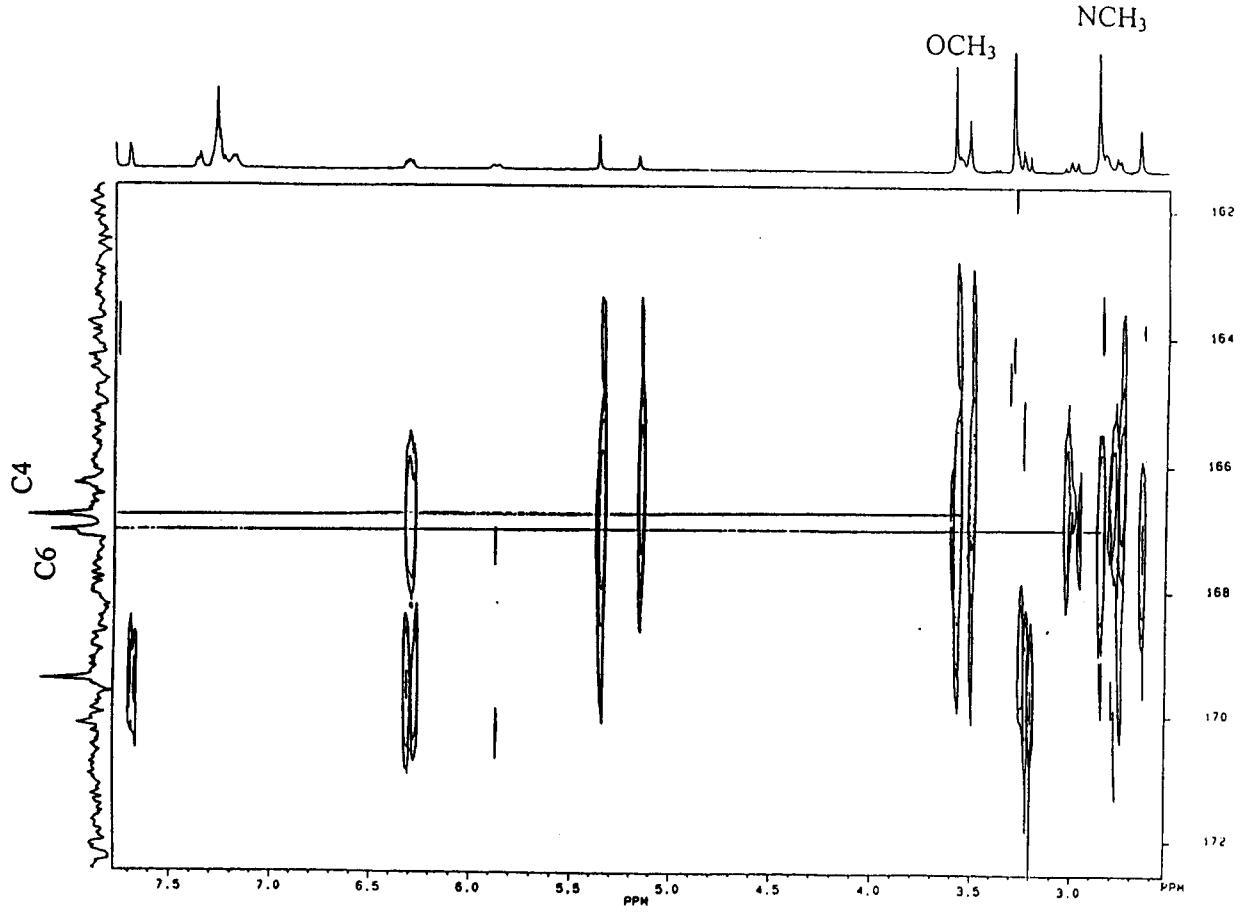

Figure 4.6 HMBC natural abundance spectrum of barbamide[40] (Expanded Region δ = 161-173 ppm)

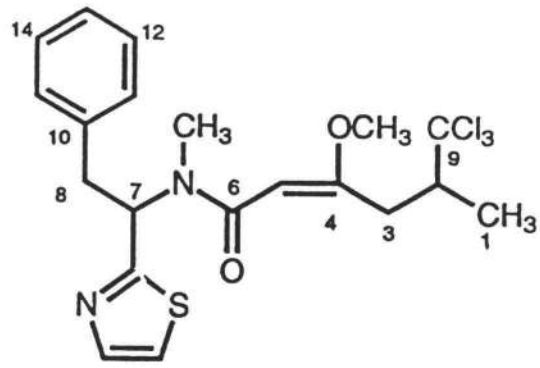

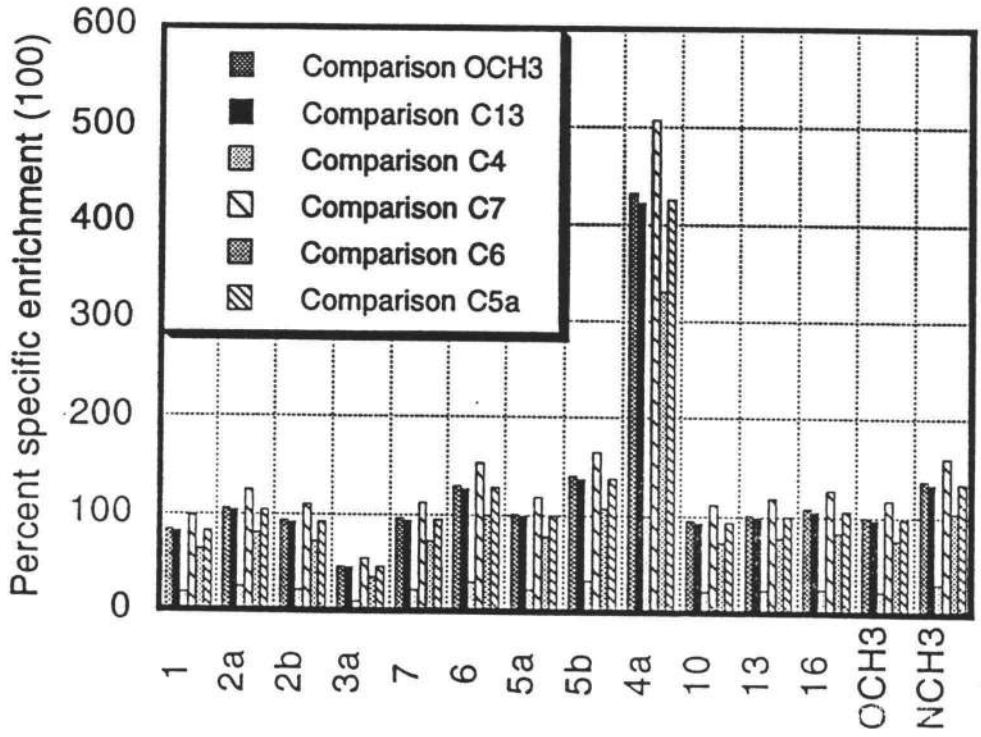

Figure 4.7 Comparative analysis of ^{13}C NMR signal intensity of leucine labeled C4 and five other selected unenriched carbons in barbamide. Expected signal intensities were calculated from the natural abundance spectrum for each of the six carbons. These values were then compared to the values calculated from the ^{13}C enriched spectrum. Signals labeled (a) and (b) are components of alternate conformations of barbamide observed in the spectrum.

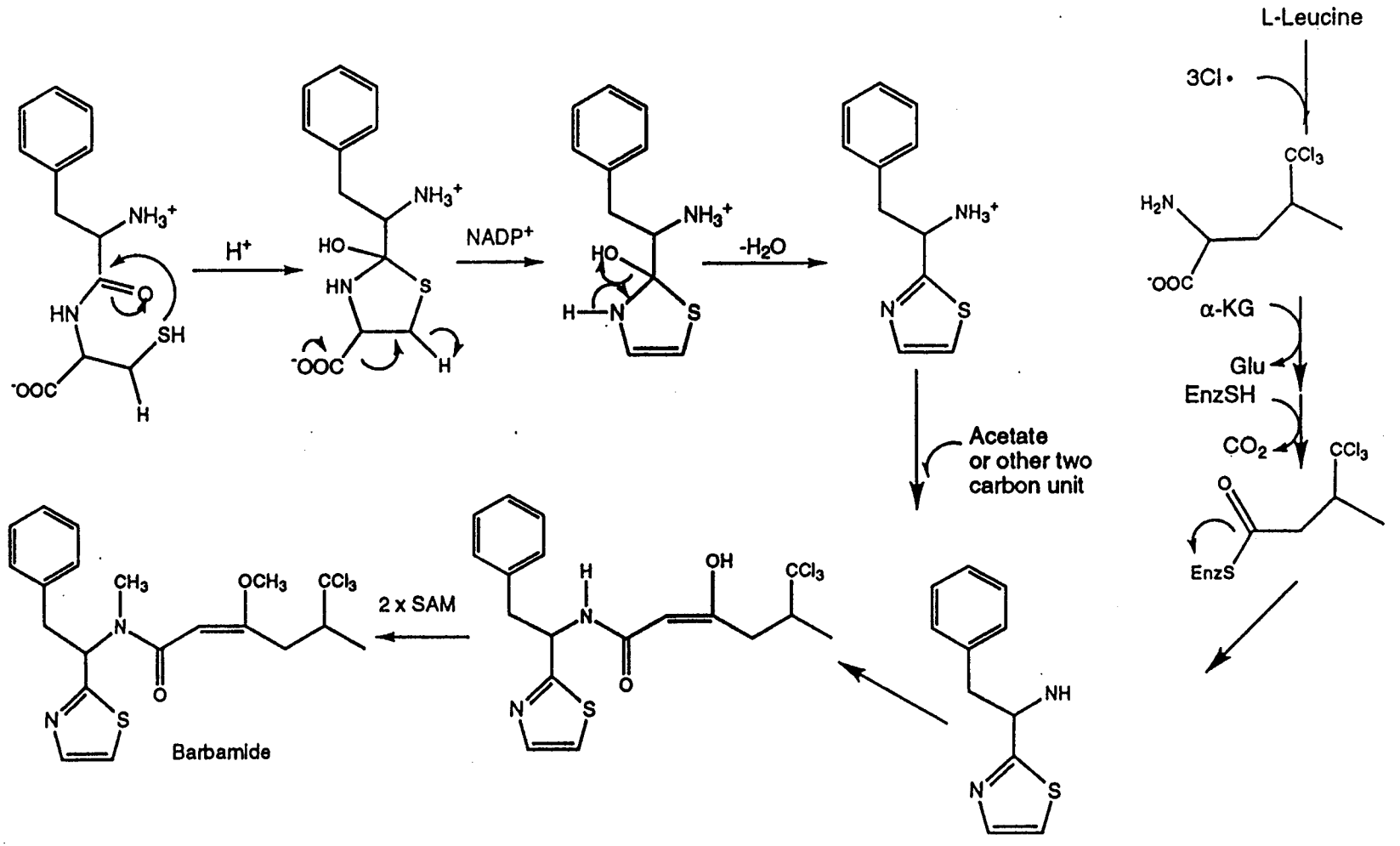

Figure 4.8 Revised proposal of the biosynthesis of barbamide from primary precursors

Elucidation of the remaining steps in the pathway are continuing in our laboratory. Recently, [3-^{13}C]-L-phe was shown to specifically enrich barbamide at a level of 2.2%.[46] This result supports our original proposal that the phenyl ring originates from this amino acid. Additional feedings are scheduled which include stereospecifically labeled leucine, and possibly a repeat of the [methyl-^{13}C]-methionine feeding.

CHAPTER 5: CONCLUSION

Over 65 distinct secondary metabolites have been isolated from *Lyngbya majuscula* since 1975. Most of these posseses biological activity whether it be selective cytotoxicity in tumor cell lines, antimicrobial activity, or general toxicity to a test organism. These properties obviously could be of great utility in biomedical and agricultural research. Less certain however, is what benefits do the production of these diverse metabolites impart to *L. majuscula*. Light is currently being shed on the role of some microbial secondary metabolites as chemical communicants in signal transduction pathways. In this capacity unique compounds could serve a variety of regulatory purposes which may facilitate adaptation to certain environmental changes. Cyanobacteria so far have not been the topic of these studies; however with the shear number and diversity of metabolites present in some species, it seems possible that this chemistry may be more than a strategy of chemical deterrence of competitors and predators. More in-depth examination of these organisms in their natural habitat and in culture will surely uncover some of these secrets.

Studies of primary metabolism in cyanobacteria, including the discovery of an interrupted TCA cycle and the presence of a nonmevalonate pathway to IPP/DMAPP, complement secondary metabolite pathway research and may be central to the unique nature of the natural products isolated from these organisms.

Although cultured *L. majuscula* has a slow growth rate in culture relative to other cyanobacteria, production yields of curacin A at approximately 10% of the crude lipid extract prove this to be an appealing alternative source to chemical synthesis. Explorations of culture conditions for the growth of several types of cyanobacteria continue to show relevance in ongoing biomedicinal, ecological, and nutritional research. Using the data presented herein regarding growth production of curacin A, culture conditions and scale-up culture, a California based biotechnology firm is endeavoring to scale-up cultures of *L. majuscula* using bioreactor methodology for the production of this metabolite.

Our isolate of *L. majuscula* strain 19L produces the compounds barbamide and curacin A, both in quantities which were sufficient to perform insightful biosynthetic studies. Although investigations of these pathways are still not complete, key elements of each scheme have been revealed. Curacin A was shown to originate from polyketide assembly. Further, the direction of this acetate polymerization indicates a probable cysteine-initiated assembly. The lipid portion was determined to arise entirely from acetate with two methylations mediated by SAM. Results of the labeled [2-^{13}C]-leucine feedings caused us to restructure our biogenetic proposal for both metabolites, curacin A and barbamide. For curacin A, this amino acid was clearly not a precursor to the cyclopropyl moiety. Incorporation of leucine into barbamide identified the amino acid rather than pyruvate as the species that is chlorinated. The preliminary findings reported here are the first biosynthetic studies to be performed on a marine cyanobacterium and are certain to contribute to an evolving understanding of secondary metabolism in these creatures.

Continued determination of the pathways may forseeably provide a means to generate directed biosynthetic analogs. By these means, *in vivo* stability of curacin A may be increased, or the antitubulin properties may be altered to effect ligand binding to it's target protein. Such efforts widely depend upon the specificity of the enzymes involved at the site of interest. The natural occurrence of chemical subclasses such as the curacins, malyngamides, microcolins and lyngbyatoxins, which reflect modifications of a common structural template in each case, further support the directed biosynthetic approach.

There has recently been a growing interest in the genetic organization of polyketide, polypeptide, and lipopeptide producing microorganisms. The science of applying recombinant technology to the modular arrangement of genes that code for these structures is currently in it's beginning stages. Generation of new biologically active structures is showing great potential through the reorganization of structural genes that code for known bioactive agents.[44,45] This field of combinatorial biochemistry is certain to have an important impact on the future of drug design.

Because the distribution of *L. majuscula* is so widespread throughout the tropics, culture of other chemotypes of this cyanobacterium are likely to be achieved from field collections in the future. The cultures that have been established by our laboratory of this chemically-rich cyanobacterium represent an exciting opportunity to perform future biosynthetic studies on unique strains. In addition, elicitation research which involves presenting producing strains with agents that effect levels of metabolite generation, can provide insight into the ecological and physiological roles of these compounds.

Preliminary field studies presented herein revealed that transplants of a low level curacin A producing strain to an environment where curacin A producers are found support that these strains are stable with respect to their generation of the metabolite. Whether this reflects a fundamental genotypic difference between strains or not needs to be confirmed with further field and molecular biological experiments.

Due to an increase in development of coastal regions in tropical regions, a number of fragile reef and mangrove ecosystems are imperiled. The ability of researchers to study these systems not only as a potential source of biomedicinals, but also to gain understanding of the complex relationships that exist among their inhabitants must be weighed against the needs of struggling economies. The preservation of biodiversity in the marine environment is fundamental to our capacity to comprehend it's relevance to terrestrial life. Hints of this relevance are emerging by breakthroughs in the atmospheric, natural products, ecological, and aquacultural disciplines.

REFERENCES

1. Giovannoni, S. J., S. Turner, G. J. Olsen, S. Barns, D. J. Lane, and N.R. Pace, *J. Bacteriology*, (1988) 3584-3592.

2. Carmeli, S., R.E. Moore, G.L. Patterson, (1990), *J. Nat. Prod.* **53**:1533-1542.

3. Patterson, G.M.L., L.K. Larson and R. Moore. (1994), *Journal of Applied Phycoclogy*, **6**:151-157.

4. Carmeli, S., R.E. Moore, G.L. Patterson, and W. Yoshida, (1993), *Tetrahedron Letters*, **34**, 35:5571-5575.

5. Gerwick, W.H., Z.D. Jiang, S.K. Agarwal and B.T. Farmer. *Tetrahedron*, (1992), **48**, 12:2313-2324.

6. Proteau, P.J., W.H. Gerwick, F. Garcia-Pichel and R. Castenholz. *Experientia* (1994), **49**:825-829.

7. Jacobs, R. Grace, K.J., Castenholz, R., P.J. Proteau, W.H. Gerwick, F. Garcia-Pichel, J.V. Rossi. Patent # 5,498,405 issued March 12, 1996.

8. Geitler, L., *Cyanophyceae*, (1930-32), Reprint (1985), Koeltz, Germany, 1028-1067.

9. Van Den Hoek, C., D.G., Mann and H.M. Jahns, (1995) *Algae: An Introduction to Phycology*. Cambridge, U.K., 33-34.

10. Gerwick, W.H., P. J. Proteau, D. G. Nagle, E. Hamel, A. Blokhin, and D Slate. 1994.*J. Org Chem.* 59:1243-45.

11. Blokhin, AV., Yoo, H.D., Geralds, R.S., Nagle, D.G., Gerwick, W.H. and E. Hamel, (1995), *Molecula Pharmacology*, **48**:523-531.

12. Koehn. F.E., R.E. Longley, and J.K. Reed, (1992), *J. Nat. Prod.*, **55**, 5:613-619.

REFERENCES (Continued)

13. Mann, J. (1994), in *Chemical Aspects of Biosynthesis*, Oxford Chemistry Press, New York 19-30.

14. Kleinkauf, H. and Von Dohren, H., (1995), *J. Antibiotics*, 48, 7:563-567.

15. Gallon, J.R., P. Kittakoop and E.G. Brown, (1994), *Phytochemistry*, **35**, 5:1195-1203.

16. Hyde, E.G. and W. Carmichael, (1991) *J. Biochem. Toxicology*, 6, **3**:195-200.

17. Moore, R.E., J.L. Chen, B.S., and G.M. Patterson, *J. Am. Chem. Soc.*, (1991), **113**, 5083-5084.

18. Armstrong, J.E., K.E. Janda, B. Alvarado, and A.E. Wright, (1991), *Journal of Applied Phycology*, **3**:277-282.

19. White, J.D., T. Kim, & M. Nambu, *J. Am. Chem. Soc.* (1995) 117:5612-13.

20. Hoemann, M.Z., Agrios, K.A., Aube, J. *Tetrahedron Lett.* (1996) 37:953-956.

21. Ito, H. Imai, N., Takao K., Kobayoshi, S., *Tetrahedron Lett.* (1996) 37:1799-1800.

22. Lai, J-Y., Yu, J., Mekonnen B., Falck, J.R., *Tetrahedron Lett.* (1996) 37:7167-7170.

23. Onada T., Shirai, R., Koiso, Y., Iwasaki, S., *Tetrahedron Lett* (1996) 37:4397-4400.

24. Onada T., Shirai, R., Koiso, Y., Iwasaki, S., *Tetrahedron* (1996) 52:14543-14562.

25. Wipf, P., and Wenjing, X., *J. Org. Chem.* (1996), 61:6556-6562.

26. Castenholz, R.W. (1988) *Methods in Enzymology*, L. Packer and A.N. Glazer (eds) **167**:68-95.

REFERENCES (Continued)

27. Rossi, J.V., M.A. Roberts, H.D. Yoo, and W.H. Gerwick, *Journal of Applied Phycology.* (In Press)

28. Bergey's Manual of systematic Bacteriology, vol. 3. (1989) James T. Staley, ed., Williams and Wilkins, Baltimore MD, 1719.

29. Bassam, J.A. and S.E. Taylor, *Methods in Enzymology*, **167**, (1988), 539.

30. Glazer, A.N. *Methods in Enzymology*, **167**,(1988), 291-304.

31. Katoh, S. *Methods in Enzymology*, **167**,(1988), 263-268.

32. Stainer, R.Y. and G. Cohen-Bazire, (1977) *Annu. Rev. Microbiol.* **31**: 225-274.

33. Smith, A.J., in "The Biology of Cyanobacteria", N.G. Carr & B.B. Whitton (Ed). (1982) 19:47-86.

34. Schwender, J., M. Seemann, H.K. Lichtenhaler, and M. Rohmer (1996) *Biocehm. J.*, 316:73-80.

35. Yoo, H.D. and W.H. Gerwick, Journal of Natural Products (1995), **58**, 12:1961-1965.

36. Marquez, B and W.H. Gerwick (work in progress)

37. Vederas, J.C., *Nat. Prod. Rep.* (1987), 321-328.

38. Voet, D.and J. Voet, (1996) in *Biochemistry*, 2nd ed., John Wiley & Sons, New York.

39. Schwender, J., M. Seemann, H.K.Lichtenhaler, and M. Rohmer (1996) *Biocehm. J.*, 316:73-80.

REFERENCES (Continued)

40. Orjala, J., D.G. Nagle, V.L. Hsu, and W.H. Gerwick, (1995), *J. Am. Chem Soc.* **117**:8281-8282.

41. Butler, A., and J.V. Walker, (1993), *Chem. Rev.*, **93**:1937-1944.

42. Norton, R.S., K.D. Croft and R.J. Wells, (1981), *Tetrahedron* , **37**:2341-2349.

43. Faulkner, D.J. and M.D. Unson, (1993) *Experientia*, 49:349-353.

44. Kao, C.M., Pieper, R., Cane, D.E., and Khosla, C., *Biochemistry*, (1996), 35, **38**:12363-12368.

45. Fu, H., Alvarez, M.A., Bailey, J.E., and Khosla, C., *Biochemistry*, (1996), 35, **21**:6527-6532.

46. Sittachita, N. and W.H. Gerwick, unpublished results.

APPENDICES

APPENDIX A

Journal of Natural Products
Vol. 57, No. 12, pp. 1717-1719, December 1994

ABSOLUTE STEREOCHEMISTRY OF NEOHALICHOLACTONE FROM THE BROWN ALGA *LAMINARIA SINCLAIRII*

PHILIP J. PROTEAU,

College of Pharmacy

JAMES V. ROSSI,

Department of Biochemistry and Biophysics

and WILLIAM H. GERWICK*

College of Pharmacy and Department of Biochemistry and Biophysics, Oregon State University, Corvallis, Oregon 97331

ABSTRACT.—Phytochemical analysis of an extract from the brown alga *Laminaria sinclairii* led to the isolation of neohalicholactone, a cyclopropyl-containing oxylipin previously isolated from a marine sponge, *Halichondria okadai*. Unequivocal stereochemical analysis of the C-15 hydroxyl group showed this isolate to be of opposite overall absolute stereochemistry compared to that proposed for halicholactone, a related compound from the sponge, and by our inference, sponge-derived neohalicholactone. Comparison of chiroptical data for all three compounds indicates the absolute stereochemistry of the sponge compounds is most probably opposite to that previously proposed.

Laminaria sinclairii (Harv.) Farl., Anders. & Eaton (Laminariaceae) has recently been shown in our laboratory to produce a variety of interesting oxylipins, including several hydroxy acids and three novel divinyl ethers (1). However, careful scrutiny of several minor fractions obtained during isolation of the above compounds showed one to possess a cyclopropyl-containing oxylipin. Following isolation of this compound by hplc, spectroscopic analysis (Experimental) showed it to be identical in overall structure and relative and absolute stereochemistry to neohalicholactone [**1**][1], an oxylipin originally isolated from the marine sponge *Halichondria okadai* Kadota along with the related metabolite halicholactone [**2**] (2,3). Our proposed biogenesis for halicholactone and neohalicholactone (4) (Figure 1) suggests that the C-15 stereochemistry is introduced via a lipoxygenase in the first step of the biogenetic pathway. We have previously shown that the putative 15-lipoxygenase of *Laminaria* spp., including *L. sinclairii*, introduces a C-15 hydroxyl function of *S* stereochemistry (1). In the original report on oxylipins **1** and **2** from *H. okadai*, a 15*R*-stereochemistry was deduced for halicholactone (2). Hence, it was of interest to unequivocally determine the absolute stereochemistry at C-15 in this algal isolate of neohalicholactone, and to consider our results in the context of the earlier stereochemical studies.

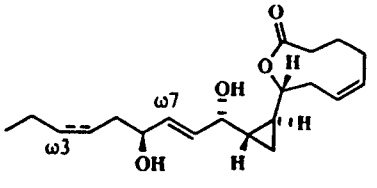

1 ω3
2 ω7

The absolute stereochemistry at C-15 in our isolate of neohalicholactone was determined by converting **1** to its corresponding (−)-menthoxycarbonyl (MC) derivative (5), oxidative ozonolysis to release the C-14 to C-17 fragment, and derivatization of this fragment to the bismethyl ester. Gc standards for this same

[1]Comparison of the authentic ^{1}H- and ^{13}C-nmr spectra for *H. okadai*-derived neohalicholactone and *L. sinclairii*-derived neohalicholactone showed them to be identical.

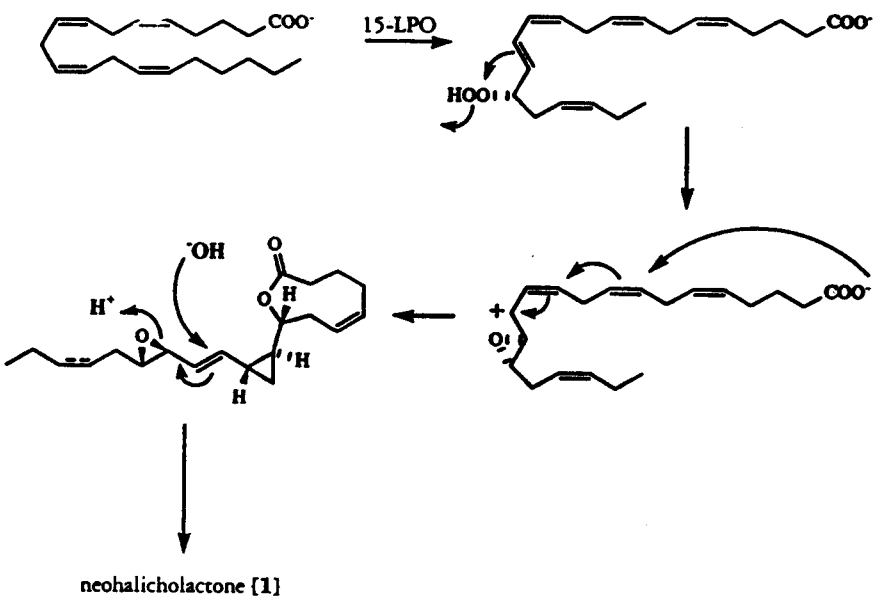

FIGURE 1. Proposed biogenesis of neohalicholactone [1].

MC derivative, as obtained from the authentic *R* and *S* malates, gave baseline separation under optimized conditions (Experimental). Under these conditions, the neohalicholactone-derived malate fragment analyzed as essentially 100% *S*, and hence *L. sinclairii* neohalicholactone is overwhelmingly of 15*S* stereoconfiguration, in opposition to that reported for halicholactone (2), and by our inference, that for sponge-derived neohalicholactone (3). Because the optical rotation of our isolate of neohalicholactone ($[\alpha]^{27}D$ −77°), is the same sign and of similar magnitude to that reported (2) for the sponge isolate of neohalicholactone ($[\alpha]^{16}D$ −54.2°), we conclude that the absolute stereochemistry in both the alga-derived and sponge-derived neohalicholactone, and likely in that of halicholactone ($[\alpha]^{23}D$ −85.4°), is 8*R*, 9*S*, 11*S*, 12*S*, 15*S*. This result is opposite that previously proposed for the sponge compounds (2).[2]

[2]Determination of the 15*R* stereochemistry in halicholactone [2] was based on measurement of a small optical rotation for a halicholactone-derived fragment (2).

EXPERIMENTAL

GENERAL EXPERIMENTAL PROCEDURES.—Nmr data were collected on a Bruker AC 300 spectrometer at 300 MHz for ^1H and at 75 MHz for ^{13}C DEPT. All shifts were reported with respect to residual solvent (C_6D_6=7.20 ppm; $CDCl_3$=77.0 ppm). Optical rotations were measured on a Perkin Elmer model 141 polarimeter. Ir data were collected on a Nicolet 510 spectrometer. A high-resolution electron impact mass spectrum (hreims) was recorded on a Kratos MS 50 TC. Hplc was run with a Waters M6000 pump, Rheodyne 7010 injector, and a Waters ri detector. Gas chromatography-electron impact mass spectrometry (gc-eims) was performed on a Hewlett-Packard 5890 series II gc connected to a Hewlett-Packard 5971 mass spectrometer. Tlc was run on Merck aluminum-backed normal-phase tlc sheets.

PLANT MATERIAL.—*L. sinclairii* was collected from mid-intertidal rocks in May 1990 at Strawberry Hill on the Oregon coast. A voucher specimen (SH-25May90-3) is on file at the College of Pharmacy, Oregon State University, and is available through W.H.G.

EXTRACTION AND ISOLATION.—The alga (2.5 gallons) was frozen on site in CO_2(s) and later stored at −20°. Blades and thalli of the plant material (640 g dry wt) were allowed to sit overnight in 2:1 $CHCl_3$-MeOH and then filtered through cheesecloth. This initial extraction was followed by two additional extractions during which the algae/solvent mixture was gently heated. All extracts were combined and concentrated *in*

vacuo to yield 7 g of a viscous brown oil. The crude extract was separated using vacuum chromatography on normal-phase tlc grade Si gel. The EtOAc to hexanes ratio was steadily increased and the column was rinsed with MeOH. Of the 14 fractions (200–250 ml each), polar fraction 12 (100% EtOAc) showed on tlc several blue-charring compounds upon heating with H_2SO_4. This fraction was further separated by Sephadex LH-20 chromatography using EtOAc-MeOH (1:1) as eluent. Fractions 9–13 of this latter chromatography (100–140 ml elution volume) contained most of the blue-charring compound and were recombined. ^{1}H-Nmr analysis showed this recombined material to possess a cyclopropyl ring-containing compound and was further separated, following methylation (CH_2N_2, Et_2O) to aid removal of contaminating fatty acids, by repetitive flash chromatography (2×, Merck Kieselgel 60, 230–400 mesh, gradient of 50–100% EtOAc/hexanes). The fractions containing this blue-charring compound were again recombined and further purified by hplc (Maxsil 10 μm, 1×50 cm, 20% *i*-PrOH/hexanes). Hplc fraction 2 contained the majority of the new compound, neohalicholactone [1] (1.3 mg), which was characterized by spectroscopic methods.

Determination of Absolute Stereochemistry of Neohalicholatone [1].—An aliquot of the neohalicholactone (200 μg) was reacted with 20 μl (−)-menthyl chloroformate in 50 μl toluene and 10 μl pyridine for 30 min. Solvents were removed *in vacuo* and the residue was resuspended in 10% EtOAc in hexanes. The reaction products were purified from polar materials over a short column of Si gel. The (−)-menthoxycarbonyl (MC) derivative was ozonized for 10 min in CH_2Cl_2 (−10°) followed by treatment with peracetic acid at 50° overnight. The reaction mixture was evaporated and the residue resuspended in MeOH and methylated with ethereal CH_2N_2. The methylated derivative was examined by gc-eims and gc (25 m, HP Ultra-1, 130–190° at 2.0° per min, then isothermal for 15 min) and compared to the corresponding *R*- (39.51 min) and *S*-malate (39.28 min) standards.

Neohalicholactone [1].—Pure 1 showed the following data: $[\alpha]^{27}D$ −77° (*c*=0.14, $CHCl_3$); hreims observed *m/z* $[M-18]^+$ 316.2038 (0.3 mmu error for $C_{20}H_{28}O_3$); gc-eims of trimethylsilyl ether derivative of 1 (method of formation as in Ref. 1) observed *m/z* $[M-69]^+$ 409 (14, $M-C_5H_9$), 319 (8), 309 (15), 307 (10), 279 (5), 243 (18), 129 (18), 73 (100); ir (film) ν max 3409, 1737, 1717 cm^{-1}; ^{1}H nmr (300 MHz, C_6D_6) δ 5.73–5.74 (2H, m, H-13, -14), 5.53 (1H, m, H-18), 5.42 (1H, m, H-17), 5.40–5.46 (2H, m, H-5, -6), 4.38 (1H, ddd, *J*=12, 8.9, and 1.3 Hz, H-8), 4.00 (1H, m, H-15), 3.56 (1H, m, H-12), 2.39 (1H, m, H-4a), 2.34 (1H, m, H-7a), 2.27 (2H, m, H_2-16), 2.12 (2H, m, H_2-2), 1.97 (2H, m, H_2-19), 1.92 (1H, m, H-7b), 1.79 (1H, m, H-4b), 1.59 (2H, m, H_2-3), 1.07 (1H, m, H-11), 0.93 (3H, t, *J*=7.5 Hz, H_3-20), 0.87 (1H, m, H-9), 0.48 (1H, ddd, *J*=8.6, 4.8, and 4.8 Hz, H-10a), 0.30 (1H, ddd, *J*=8.6, 4.8 and 4.8 Hz, H-10b); ^{13}C nmr DEPT 135 (75 MHz, $CDCl_3$) δ 135.4 (C-14, +), 134.7 (C-13, +), 133.3 (C-17, +), 131.9 (C-5, +), 124.6 (C-6, +) 123.6 C-18, +), 76.1 (C-8, +), 74.2 (C-12, +), 71.6 (C-15, +), 35.2 (C-16, −), 33.8 (C-7, −), 33.6 (C-2, −), 26.5 (C-4, −), 25.3 (C-3, −), 23.4 (C-11, +), 20.7 (C-19, −), 19.5 (C-9, +), 14.2 (C-20, +), 8.2 (C-10, −).

ACKNOWLEDGMENTS

We thank Elizabeth Barofsky of the Oregon State University College of Agricultural Chemistry for hrms measurements. We thank Professor K. Yamada, Nagoya University, for providing authentic spectra of neohalicholactone. This work has been supported by the Oregon Sea Grant Program (R/SH-5) and NIH (CA 52955).

LITERATURE CITED

1. P.J. Proteau and W.H. Gerwick, *Lipids*, 28, 783 (1993).
2. H. Niwa, K. Wakamatsu, and K. Yamada, *Tetrahedron Lett.*, 30, 4543 (1989).
3. H. Kigoshi, H. Niwa, K. Yamada, T.J. Stout, and J. Clardy, *Tetrahedron Lett.*, 32, 2427 (1991).
4. W.H. Gerwick, D.G. Nagle, and P.J. Proteau, in: "Topics in Current Chemistry, Vol. 167." Ed. by P.J. Scheuer, Springer-Verlag, Berlin 1993, pp. 117–180.
5. M. Hamburg, *Anal. Biochem.*, 43, 515 (1971).

Received 26 April 1994

APPENDIX B: SYNTHETIC MODIFICATIONS OF SCYTONEMIN

The indole alkaloid scytonemin (**1**) (figure B.1) has been recognized as a powerful antiinflammatory agent. The compound originally isolated from a *Scytomena* sp., also possesses photoprotectant properties which may be applicable as a sun screen agent. These two important characteristics have merited closer evaluation of scytonemin for use either topically or systemically in humans.

Two undesirable properties of the alkaloid which have hindered further development are its intense green/brown color and insolubility in aqueous and limited solubility in many organic solvents. The pigmented nature of the agent make it an unattractive candidate for topical application while the insolubility would certainly limit its *in vivo* bioavailability.

Tetrahydrodrofuran has been observed to solubilize the compound most efficiently. Other organic solvents that have been used are in order of decreasing solubility; pyridine > DMF > acetone. The agent is insoluble in hexane, Et_2O, H_2O, EtOH, MeOH, and EtOAc and only sparingly soluble in $CHCl_3$.

Early studies showed that the agent is easily reduced in the presence of a 2:1 molar ratio of ascorbic acid to scytonemin in THF. This yields reduced scytonemin (**2**) which is burgundy in color and has slightly increased solubility in EtOAc and acetone.[6] Reduced scytonemin possesses less antiinflamatory activity then it's oxidized counterpart.

Scytonemin, which naturally occurs as a dimer, contains two phenolic groups that could possibly be modified in order to ameliorate these characteristics. In the following study, attempts were made primarily to increase the compounds solubility and secondarily to alter its pigment nature. Reactions were aimed at the methylation and acetylation of the phenolic hydroxyl groups.

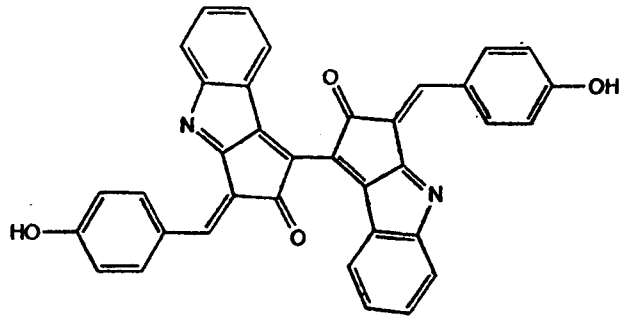

1

scytonemin

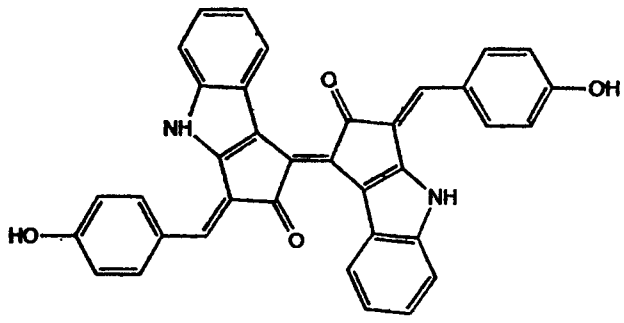

2

reduced scytonemin

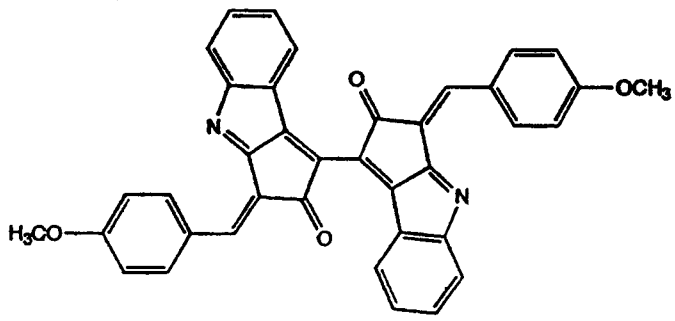

3

scytonemin dimethyl ether

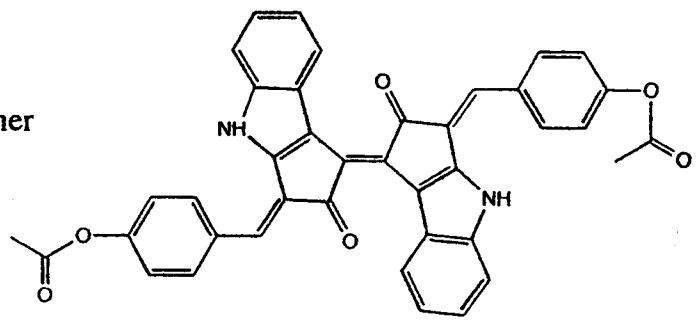

4

scytonemin diacetate

B.1 Structures of Scytonemin and it's Derivatives

Experimental

Methylation of scytonemin: CH_3I (77.5 mg) was reacted with 29.3 mg scytonemin and 28.0 mg K_2CO_3 in 7.0 mL THF. The reaction proceeded in a conical vial with constant stirring at room temperature for 24 hrs. Reaction progress was monitored by TLC using aluminum backed silica plates and 10% MeOH/$CHCl_3$ as the mobile phase. Separation of the reaction products was achieved by using preparative TLC in 5% MeOH/$CHCl_3$. Three bands were scraped from the plate and collected separately. The highest band (R_f approx 75) was assumed to be the dimethyl ether derivative. The silica containing this band was rinsed with THF in a Buchner funnel fitted with paper filter. Product mass was 14.0 mg.

Acetylation of scytonemin: Scytonemin (11.0mg) was reacted with 0.5 mL of acetic anhydride in 3 mL of pyridine. The reaction was stirred for 16 hrs. Products of the reaction were assessed by silica TLC in 10% MeOH/$CHCl_3$. A gold precipitate formed in a deep red solution. The solid was filtered onto paper (Whatman) and the red filtrate was collected. Mass of the solid was 8.3 mg and was confirmed to be the diacetate of scytonemin by 1H NMR run at 300 Mhz in $CDCl_3$. FAB-MS was also used to confirm the structure.

Results

Reaction of scytonemin (M_w = 546) with CH_3I gave a mixture of products which were the mono- and dimethyl phenolic ethers. By preparative TLC the highest R_f band was identified as the dimethyl ether of scytonemin. FAB-MS showed an M+1 ion of m/z = 575 which is consistent with substitution of two methyl groups for the two phenolic protons. The ^1H NMR spectrum showed an additional signal at δ = 3.75 ppm (not present in the spectrum of scytonemin) which was assigned to the phenolic methyl groups. UV

spectrophotometry revealed that the λ_{max} = 386 nm had not greatly changed from that of the starting material.

The color of this compound was a lighter shade of green but was not greatly changed. The dimethyl ether (**3**) was slightly more soluble then the starting material in acetone and $CHCL_3$ at around 10 mg/mL.

Scytonemin diacetate (**4**) was formed from the reaction of acetic anhydride and scytonemin. This appeared as a gold "metallic" looking residue which coated the reaction vial. Reduced scytonemin was present as a reaction product which remained in the pyridine solution. Scytonemin diacetate had decreased solubility in THF and pyridine but was totally soluble in $CHCl_3$ and DMF. The ^1H NMR spectrum of the compound showed an additional singlet at δ = 2.23 ppm which was assigned to the methyl adjacent to a carbonyl in an acetyl functionality. Confirmation of the diacetate structure was provided by FAB-MS which gave an M^+ as m/z = 630 amu. This is consistent with the acetylation of the reduced scytonemin. The λ_{max} in the UV spectrum was shifted to λ_{max} = 350 nm.

Both scytonemin dimethyl ether and scytonemin diacetate have been evaluated for their antiinflammatory activity and found to be of a lesser potency in comparison to the parent compound. Neither compound possessed greatly improved solubility characteristics.